RESEARCH REPORT 2015-21

APEC CLIMATE CENTER

Application of the Regional Rice Model GLAM-Rice in the Seasonal Crop Forecasting of South Korea

Sanai Li
Climate Change Research Team

APCC
APEC CLIMATE CENTER

APEC CLIMATE CENTER
RESEARCH REPORT

Application of the Regional Rice Model GLAM-Rice in the Seasonal Crop Forecasting of South Korea

Sanai Li
Climate Change Research Team

RESEARCH REPORT 2015-21

APCC
APEC CLIMATE CENTER

Preface

Climate change and weather are important factors affecting agriculture variability. Seasonal crop forecast is critical to examine whether crop yield and yield risk are stable, enhancing or declining in advance so that it can provide early warnings and make decision support early. A large number of previous studies have used the site based dynamic crop models to forecast crop production at a regional scale, and although the results have been promising, few studies have led to operational forecasting systems due to the spatial scale mismatch between climate model output and input requirement in crop model. The general large-area model (GLAM) for annual crops has been designed to operate at the spatial scale of global and regional climate models, which provides a useful tool to forecast crop yield directly at the regional scale.

The APEC Climate Center (APCC) is responsible for providing seasonal climate forecasts and climate information services in the Asia-Pacific region, and supports for its application in various sectors such as agriculture to help farmer and other agricultural stakeholders to manage risk and improve decision making. So developing a combined crop and climate forecast system is an effort of APCC for the regional scale decision-makers needs.

The objectives of this study are to find the appropriate spatial and temporal scales of weather data required in the crop model to make an improvement in the forecast accuracy and to develop methods for using the multi-model ensemble seasonal forecast in the crop model, and find ways to further improve the crop forecast so that it becomes more reliable when applied on a large spatial area. Section 3.1 and section 3.2 show how input data accuracy and the temporal and spatial scale of input data affect the forecast skill of crop model. Section

3.3 shows the application regional crop model in seasonal crop forecasting by driving the crop model with the APCC's seasonal climate forecasts.

This study is expected to find the skill to further improve the crop forecast so that the crop model becomes more reliable when applied on crop forecast a large spatial area. These results also provided prior evidence on how to apply APCC's seasonal climate forecasts in crop model, and consequently it will provide support evidence for developing the operational seasonal crop forecast system. This case study would provide useful evidence of the value of simulation models in forecasting crop performance.

The APCC would like to express its gratitude to all staff members at our institute and the researchers who have contributed to this publication.

Dr. Chin-Seung Chung
Director / APEC Climate Center
March 2015

ABSTRACT

Reliable crop forecasts can provide an early warning and decision support for farmers and other agricultural stakeholders for better risk management and improved decision-making. A number of studies have used dynamic crop models to forecast crop production at a regional scale with promising results, few studies have led to operational forecasting systems due to limitations in data availability and the inaccuracy of input data. A general large-area model (GLAM) for rice has been developed, which provides a useful tool for forecasting rice yield directly on the regional scale. However, the forecast skill of GLAM-Rice is affected by the accuracy of the input dataset and its calibration methods, and the spatial and temporal scale used. It is possible to use the monthly average rainfall in the crop model for a rice yield forecast, accurate daily temperature and solar radiation are required. The forecast skill of the GLAM-Rice was higher at the national level than for individual grid cells, because when a forecast was conducted over a larger spatial scale, the errors from different sources could be offset by each other. While forcing the GLAM-Rice with the six-month seasonal forecasts, the forecast skill improved with successive monthly updates using observations. The forecast skill of the GLAM-Rice has a higher association with solar radiation than with temperature. It is therefore to conclude that if reliable solar radiation data could be provided, it would be feasible to use properly downscaled multi-model ensemble seasonal forecasts from GCMs for predicting crop yields earlier in the crop growing season.

Contents

Application of the Regional Rice Model GLAM-Rice in the Seasonal Crop Forecasting of South Korea

1. INTRODUCTION

The application of crop yield monitoring and forecasting on regional, national, and sub-national scales is receiving increased attention in both developing and developed countries (Bouman et al. 1995). Reliable crop forecasts can provide early warnings and decision support for farmers and other agricultural stakeholders in relation to managing risk and improving decision making. Extreme weather events are expected to increase with the rise in global temperature, and therefore improvements in methods of predicting crop yields are important for helping stakeholders to make advances in-season crop management and financial decisions (IPCC 2013).

Statistical regression methods and dynamical crop models are the most widely used methods for forecasting crop yield. Statistical models use previously observed empirical relationships between climate and yield to forecast crop yield, and are often the preferred methods for crop forecasting due to their low data requirements and simplicity of implementation (Becker-Reshef et al. 2010). However, statistical regression models are limited by the non-linear response of crops to their environment (in particular, extreme climate events) (Semenov & Porter 1995, Porter & Semenov 1999, 2005) and the forecast model is only valuable for the range and area for which it has been calibrated (Doraiswamy et al. 2003). In contrast, dynamic crop models seek to simulate the complex processes between crop growth, development, and its response to environmental variables. If reliable weather information (observed conditions and weather forecasts) can be provided, crop simulation models could be the most promising way to forecast crop yield (Nichols 1991; Abawi et al. 1995). A traditional crop model is mostly designed to simulate crop yield based on the specific-site level. For example, processed-based models such as the Wageningen model (Van Ittersum et al. 2003), DSSAT (Jones et al. 2003), STICS (Brisson et al. 2003), CropSyst (Stöckle et al. 2003) and APSIM (McCown et al. 2003) have been developed to successfully simulate crop growth and development at a local scale. These site-based crop models generally have a good performance in reproducing crop growth and yield at a local scale. A large number of previous studies have used dynamic crop models to forecast crop production at a regional scale (Hammer and Muchow, 1991; Rosenthal et al., 1998), and although the results have been promising, few studies have led to operational forecasting systems due to the associated limitation relating to the lack of availability and

inadequate accuracy of the input data (Chipnashi et al. 1999; Moulin and Guerif 1999), and the complexities involved in integrating detailed input parameters from the small-scale to the sub-national and national levels (Potgieter 2005).

Rice is the staple food of South Korea, and a reliable rice yield prediction would provide useful information for managing an unstable food supply on a national level (Park et al., 2012). However, only a few studies have been performed based on agriculture zone simulations using an observed historical climate dataset to predict the rice yield at a national level. For example, Park et al. (2012) used a multiple linear regression analysis between yield, meteorological elements, and NDVI extracted from satellite images to predict rice yield in 2011 for South Korea. In addition, Yun (2003) developed an area-based rice production forecasting system by scaling-up a site-based simulation from CERES-Rice to 162 crop-reporting districts, for a period of three years (1997–1999), in South Korea. However, CERES crop models have high data input requirements, and do not include yield loss in relation to pests and diseases, nor detailed field management information. Thus, detailed spatial and temporal yield variability is poorly captured by the models on a regional level. For example, at the national level of South Korea, the consistent spatial pattern ($r = 0.47$ for 1997, $r = 0.48$ for 1998, and $r = 0.28$ for 1999) between simulated and observed yields on a county scale is relatively low (e.g. Yun, 2003). Only a limited number of studies have been performed in relation to an operational seasonal crop forecast system for South Korea, and this is related to limitations in the prediction methods and the lack of availability of high-resolution seasonal climate forecasts. It is therefore considered necessary to develop an operational crop forecast system for forecasting crop yield on a regional level. A general large-area model (GLAM) for annual crops has been designed to operate at the spatial scale of both global and regional climate models (Challinor et al. 2004). The initial motivation to develop GLAM was related to the requirement to simulate crop yields directly on large spatial scales. In GLAM, although the crop yield loss due to nutrients, pests, diseases, and field management is not directly modeled, it is represented by the yield gap parameter, which allows the model to focus on the response of crop yield to spatial and temporal weather and climate variability. GLAM has the benefit of requiring minimum data sets for inputs, has validity over large areas, and has the potential of capturing the variability due to different sub-seasonal weather patterns (Challinor et al. 2004). Furthermore, GLAM is able to apply a number of simple assumptions and empirical relationships to predict complex

crop growth and development. The simplified model formulation makes it possible to input less crop parameters, and GLAM can then be operated on a relatively larger spatial scale; the model has been successfully used to simulate groundnut yield over large areas in India (e.g. Challinor et al. 2004). The GLAM model has been linked with DEMETER hindcast weather ensembles to simulate the probabilistic distribution of crop yield over India, and it has shown predictive skills in both the ensemble mean and the ensemble spread (Challinor et al. 2005).

The GLAM model has been designed to allow modifications for various crops by modifying the crop-specific parameters and a number of specific growth and development processes. A large-scale wheat model has been developed using the GLAM framework to assess the potential for large-area modeling of wheat in China. Based on the existing GLAM-Wheat model, the GLAM-Rice model was developed by Li (2013) through defining rice growth and developmental parameters, and quantifying a number of rice growth and developmental processes, which provides a method for forecasting rice yield directly on a regional level. This in turn will permit the forecast of rice productivity directly on a regional level. However, temporal and spatial scales of climate variables can have a great impact on the skill of GLAM for rainfed crop such as wheat in China (Li and Tompkins 2012), and the reliability of crop forecasts depends on the accuracy of climate variables, the crop model itself and the related temporal and scales. How the temporal and spatial scales of climate variables affect the forecast skill of the GLAM-Rice, therefore, needs to be investigated to discover the appropriate climate variable scale for running the model.

Solar radiation is a key input in GLAM, and is used for estimating evapotranspiration and rainfall. Accurate solar radiation data is required for a reliable crop forecast. However, solar radiation is only measured at certain sites on a global scale. For example, in South Korea 18 stations measure solar radiation and provide records, whereas sunshine records are available from all stations (60) between 1980 and 2010 (as shown in Figure 1). As a measured climate variable, such as sunshine duration, is often used to estimate global solar radiation (Louis et al. 2003), it is also used in this study to estimate solar radiation in South Korea.

Leaf area index (LAI) is an important parameter in crop models that affects crop growth. A few studies have integrated LAI measurements derived from satellites into crop growth, to predict crop yield on a regional scales. For example, Doraiswamy et al. (2003) applied the MODIS derived LAI to calibrate the crop model parameters by adjusting the simulated LAI. In addition, Mo et al. (2005) used the LAI derived from NOAA-AVHRR as an input of crop model to predict crop yield in the Hebei Province of China. Their results showed that LAIs derived from satellites can provide useful information for forcing and updating the seasonal crop forecasting in regions with homogeneous land cover. Therefore, further investigation is required to ascertain whether satellite-derived LAIs can be used in a regional crop model for updating seasonal crop forecasts in areas with complex topography, such as in South Korea.

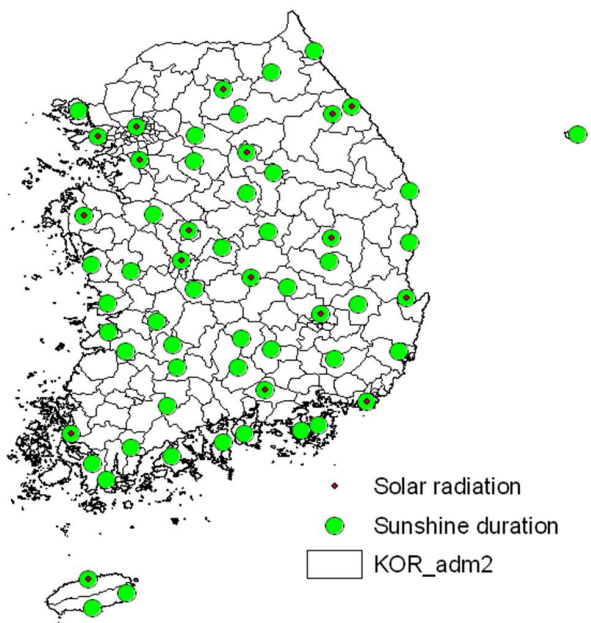

Figure 1. Locations of weather stations in South Korea; brown dots represent stations that provide solar radiation measurements, and green dots represent stations that provided sunshine duration measurements for 1980–2010.

The objectives of this study are:

(1) To estimate solar radiation using the regression equation between solar radiation and sunshine duration in South Korea from 1985–2000.

(2) To investigate how the temporal and spatial scales of rainfall and temperature affect the capabilities of the GLAM-Rice, and to find the appropriate spatial and temporal scales of weather data required in the crop model to make an improvement in the forecast accuracy.

(3) To develop methods for using the multi-model ensemble seasonal forecast in the crop model, and find ways to further improve the crop forecast so that it becomes more reliable when applied on a large spatial area.

(4) To explore the feasibility and efficiency of using satellite-derived LAI for rice yield forecasting in regions with inhomogeneous cropland cover, such as South Korea.

2. DATA AND METHODOLOGY

2.1 Research area

South Korea extends between latitudes 33° to 43°N, and between longitudes 124° to 132°E. The climate is characterized as temperate, with cold winters and hot, humid summers. Across South Korea, the average total seasonal rainfall during the rice growth season ranged from 1880 mm in the south to 880 mm in the north between 2000 and 2010 (Figure 2a), and, and the average seasonal mean temperature during rice growth season ranged from 20.7 to 23.7℃ (Figure 2b). South Korea has been selected as a case study for two reasons; firstly, because rice is the country's most important food crop, and secondly because data pertaining to both the observed rice yield and the weather are available. In South Korea, the share of agriculture added value declined from 15% of the GDP in 1980 to 5% in 2000, due to expansions in the share of industry and the service sector (http://data.worldbank.org/). In 2013, rice represented approximately 80% of crop land area and 87.5% of crop production (http://kosis.kr). There was a decline in rice production between 1988 and 2012, from about 8.2 million tons in 1988 to 5.4 million tons in 2012, mainly due to a reduction in the harvest area related to the rising costs involved in rice production, e.g., the rising costs of labor, services, farm implements, and fertilizer (Li 2013). Therefore, a combination of the growing population and the reduction in available farmland due to urbanization will ultimately ensure that the demand for food will greatly outstrip supply

(Savada and Shaw 1990). In this respect, the ability to make accurate seasonal crop forecasts is extremely important, in that it can provide information for decision making by stakeholders.

In South Korea, the main rice growing season is between May and October. Low temperature stress, which can damage the rice plant between booting and maturity, is one of the limiting factors affecting rice production, particularly in the northern mountainous regions (Lee, 2001). Rice is quite sensitive to low temperature stress between the booting and flowering stages, and the spikelet formation can be affected resulting in a lower final grain yield; therefore, increased temperatures stimulate the growth of rice and increase rice yield.

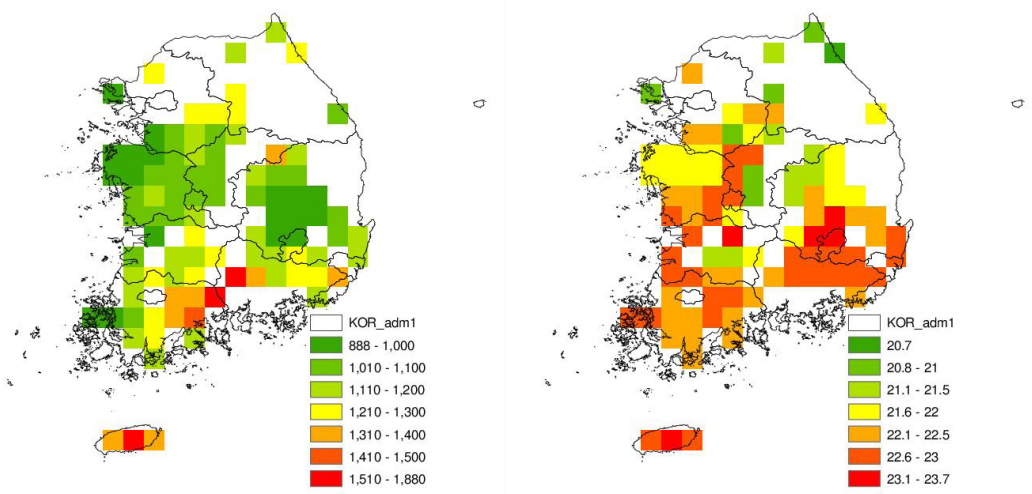

Figure 2. (a) observed average of seasonal total rainfall (mm) during the rice growth season in South Korea from 2000–2010; (b) observed seasonal mean temperature average (ºC) during the rice growth season in South Korea from 2000–2010 rainfall and temperature data were interpolated from the dataset of KMA meteorological stations.

2.2. The Crop model

2.2.1 An overview of the crop model

The dynamical model GLAM-Rice, which is a process-based regional crop model with a daily time-step simulation, is used in the study to forecast the regional rice yield. The

model simulates soil water balance, leaf canopy, root growth, biomass, and final crop yield, all of which are limited by yield gap parameters, inadequate soil water, or extremes in temperature. Figure 3 shows a flowchart of the GLAM model structure and the processes of yield and biomass formation. The detailed descriptions of crop development, crop growth, and evapotranspiration can be found in Challinor et al. (2004). In GLAM, the crop yield is simulated daily as the product of accumulated biomass and the harvest index (the ratio of grain yield to biomass). After grain-filling, the harvest index is assumed to increase linearly with time, but is limited by high temperature stress. Biomass is accumulated through transpiration and transpiration efficiency; transpiration can be affected by temperature, total solar radiation, available soil water, LAI, and root growth. For the detailed parameters used in GLAM, see Appendix A and B.

In GLAM, the above-ground biomass (W)is accumulated through actual transpiration (T_T), the least favorable transpiration efficiency ($\frac{E_T}{V}$), and the maximum transpiration efficiency ($E_{TN,max}$), as shown by Eq. 2.1:

$$\frac{\partial W}{\partial t} = T_T \min\left(\frac{E_T}{V}, E_{TN,\max}\right) \tag{2.1}$$

where W (kg ha^{-1} day^{-1}) is the daily crop above-ground biomass production; E_T (Pa) is the normalized transpiration efficiency (i.e., $V\times$ transpiration efficiency in g kg^{-1}); V(kPa) is the daily mean vapor pressure deficit (VPD = $e_{sat}(\overline{T}) - e$, where e is the vapor pressure); $E_{TN,max}$ (g kg^{-1}) is the maximum transpiration efficiency; and T_T (cm day^{-1}) is the daily actual transpiration, which is affected by the temperature, LAI, root growth, and available soil water.

$$Y = HI \times W \tag{2.2}$$

where Y is yield (kg ha^{-1}), which is produced by the harvest index, (HI), and the above-ground biomass (W).

In GLAM, the reduction of crop yield due to factors such as pests, diseases, and field management is not simulated directly, but is represented using the Yield Gap Parameter (YGP). The YGP in GLAM is a calibrated parameter, which is the ratio between the actual farm yield and the potential level. It is measured using a range from zero to one in steps

of 0.05, and is calibrated using the observed yields by minimizing the Root Mean Square Error (RMSE) between observed yields and simulated yields. As shown by Figure 4, the RMSE is a function of the yield gap parameter; for example, the RMSE is smallest when the YGP is equal to 0.5, and the optimal value of YGP is thus 0.5. Therefore, the calibration processes of the YGP is a type of mean bias-correction approach, which can be used to partially correct bias, such as the bias in input data or a crop model error (Challinor et al., 2005). In GLAM, the LAI is simulated through an LAI expansion rate, which is assumed to be constant under optimal conditions, and is reduced by sub-optimal temperatures, water stress, and the yield gap parameter.

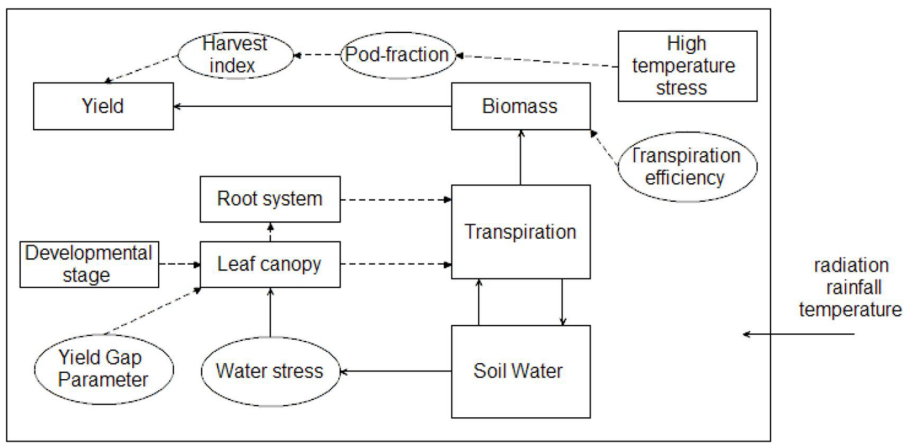

Figure 3. Flowchart of GLAM's biomass and yield growth calculations

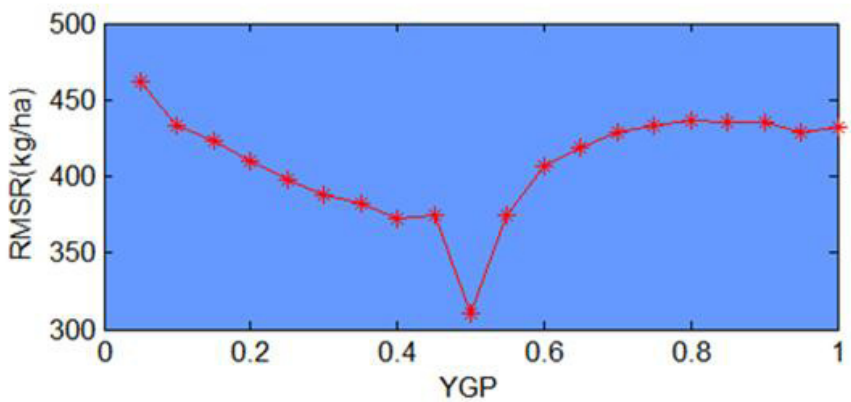

Figure 4. An example of calibration of the yield gap parameter (YGP) using GLAM, which shows the YGP between 0.05 to 1 in steps of 0.05. The root mean square error (RMSE) is a function of the YGP.

2.2.2 Crop development

The simulation of developmental stages in GLAM is controlled by accumulating daily mean values of temperature above a base temperature (the accumulated thermal time). Once the thermal time accumulation reaches the specified thermal time for a given stage, the next stage begins. The thermal time accumulation for each development stage is given by the following equation:

$$t_{TT} = \int_{t_i}^{t_{i+1}} (T_{eff} - T_b) dt \tag{2.3}$$

where t (days) is time, T_b (℃) is the base temperature below which crop development stops, i is the number of the development stage, and t_{TT} (℃d) is the thermal time accumulation. The thermal time is accumulated when the daily effective temperature (T_{eff}) exceeds the base temperature (T_b). The development stage, i, begins at time, t_i, and ends at time t_{i+1} as the thermal time accumulation reaches the specified thermal duration.

The daily effective temperature, T_{eff} (℃), is determined by the base T_b (℃), optimum T_o (℃), and maximum T_m (℃) temperatures. $\overline{T}$ (℃) is the daily mean temperature, which is given by equation (2.4):

$$T_{eff} = \begin{cases} \overline{T} & T_b \le \overline{T} \le T_o \\ T_o - (T_o - T_b)\left(\frac{\overline{T} - T_o}{T_m - T_o}\right) & T_o \le \overline{T} \le T_m \\ T_b & \overline{T} \le T_b \,,\ \overline{T} \ge T_m \end{cases} \tag{2.4}$$

When the daily mean temperature is between the base temperature and the optimal temperature, the daily effective temperature is equal to the daily mean temperature. For a mean temperature between the optimal temperature and the maximum temperature, an increase in the temperature has a decreasing effect on the effective temperature. For a temperature above the maximum temperature or below the base temperature, T_{eff} is determined by the base temperature.

Research has shown that the photoperiod and temperature can affect plant development (Yan and Wallace 1995). Rice is a short day plant, and the development rate of photoperiod-sensitive species is reduced when the day length is longer than a critical value. The daily relative photoperiod effectiveness, (R_{pe}), is affected by the photoperiod sensitivity of the

plant variety, the effective photoperiod hours, and the critical photoperiod hours. The critical photoperiod of rice is 11.5 hours, and its development rate is delayed when the day length is longer than this (Bouman et al. 2001). The daily relative photoperiod effectiveness (R_{pe}) is estimated according to the following equations:

$$D_{ec} = 0.4093 \times SIN(0.0172 \times (D_{OY} - 82.2)) \quad (2.5)$$

$$D_L = (-SIN(0.01745 \times Lat) \times SIN(D_{ec}) - 0.1047)/(COS(0.01745 \times Lat) \times COS(D_{ec})) \quad (2.6)$$

$$P_h = 7.639 \times \mathrm{ACOS}(D_l) \quad (2.7)$$

$$R_{pe} = 1 - P_s \times (P_h - C_{ph}) \quad (2.8)$$

$$TTA = \sum DTT \times R_{pe} \quad (2.9)$$

where D_{ec} (radians) is the sun declination, D_{OY} is the day of the year, D_L (hours) is the day length variable, Lat is the latitude, P_s is the photoperiod sensitivity, and P_h (hours) is the effective photoperiod hours expressed using the function from Ritchie (1991), R_{pe} is the daily relative photoperiod effectiveness, C_{ph} (hours) are the critical photoperiod hours, TTA (°Cd) is the thermal time accumulation, and DTT (°Cd) is the daily thermal time.

2.2.3 The water balance

The crop model ORYZA2000 is a widely used crop simulation model that simulates the growth, development, and water balance of lowland rice. It simulates various water balance components, such as the depth of ponded water, evapotranspiration, deep percolation, capillary rise, surface runoff, and the depth of irrigation water and groundwater at daily increments (Bouman et al. 2001). The water balance of paddy crops is different from the water balance of field crops because paddy fields require water standing in the field during the rice growth period. Therefore, the water balance model of paddy fields from the ORYZA2000 was incorporated into the GLAM to simulate the soil water balance of lowland paddy fields (Li 2013). In this respect, the GLAM firstly simulates potential evapotranspiration using the simpler Priestley-Taylor equation (Priestly and Taylor 1972), and the potential evapotranspiration is partitioned into potential transpiration and potential evaporation according to LAI and available soil water. The energy-limited evaporation and

transpiration rates (E^e and T_T^e, respectively) are described using the simpler Priestley-Taylor equation (Priestly and Taylor 1972), and the potential evapotranspiration rate is given by Eq. 2.10:

$$E_{pot}^T = E^e + T_T^e = \frac{\alpha}{\lambda} \frac{\Delta (R_N - G)}{\Delta + \gamma} \tag{2.10}$$

where R_N is the net all-wave radiation, G is the soil heat flux, λ is the latent heat of vaporization of water, $\Delta = \partial_{esat}/\partial T$ is the slope of the saturation-vapor pressure versus the temperature curve determined after Bolton (1980), γ is the ratio of the specific heat of air at a constant pressure to the latent heat of vaporization of water, and α is the Priestley-Taylor coefficient.

Light interception is estimated with the Beer-Bougert equation (e.g. Arya 1988) given by:

$$E^e = (1 - C_G) E_{\max}^T e^{-kL} \tag{2.11}$$

$$T_T^e = E_{\max}^T (1 - e^{-kL}) \tag{2.12}$$

where C_G is the constant in the equation for the soil heat flux, $G = C_G R_N e^{-kL}$ (Choudhury et al. 1987), k is the extinction coefficient, and $E_{\max}^T$ is the maximum possible energy-limited evapotranspiration, which is given by setting $G = 0$ in Eq. 2.10.

The potential energy and physiology limited transpiration rate is shown by Eq. 2.13:

$$T_{Tpot} = \min(T_{Tpot}^p, T_T^e) \tag{2.13}$$

The potential transpiration and evaporation from GLAM are used as inputs for the water balance of the ORYZA2000 model to simulate the soil water content, water stress factor, transpiration, and evaporation. The water stress factor and transpiration from the water balance of paddy fields are used in GLAM to reduce the leaf area index and transpiration. Rice is mostly irrigated in South Korean paddy fields, and therefore rice was simulated under irrigated conditions. In the GLAM-Rice, irrigation is provided when the depth of ponded water is below 10 cm. The water stress factor related to soil water tension from ORYZA2000 (Bouman et al. 2001) was applied to quantify the effect of drought stress on rice yield. The drought stress can reduce transpiration and leaf area index.

$$TRR = \frac{\log_{10} MSKPA - \log_{10} LLRT}{\log_{10} LURT - \log_{10} LLRT} \tag{2.14}$$

$$LE = \frac{\log_{10} MSKPA - \log_{10} LLLE}{\log_{10} ULLE - \log_{10} LLLE} \tag{2.15}$$

where TRR is transpiration reduced factor due to water stress; $MSKPA$ is soil water tension, which is a function of the soil water content; $ULRT$ (70kPa) and $LLRT$ (1500k Pa) are lower and upper relative transpiration; LE is the relative leaf expansion rate due to water stress; $LLLE$ (50kPa) is the lower limit of leaf expansion; and $ULLE$ (260kPa) is the upper limit of leaf expansion.

2.2.4 Temperature stress

Low and high temperature stress can affect the spikelet formation and finial gain yield of rice. As previously mentioned, rice is quite sensitive to low temperature stress between the budding and flowering stages. According to the study of Horie et al. (1992), the spikelet sterility of rice increases with an accumulation of cooling degree-days, when the daily average temperature is below a critical value (Uchijima 1976). The cooling degree-days (COLDTT; °Cd) and the percentage fertility caused by cold (S_c) are calculated as follows:

$$COLDTT = \sum_{p}^{f} (220\text{LD}) \tag{2.16}$$

$$S_c = 1 - (4.6 + 0.054 \times \text{COLDTT}^{1.56}) / 100 \tag{2.17}$$

where $COLDTT$ is the cooling degree-days, Td is the average temperature, p and f are the dates of panicle initiation and flowering, and S_c is the percentage sterility caused by cold.

Even short episodes of high temperature can have a dramatic impact on crop yield, especially at anthesis, when plants are vulnerable to high temperature stress (Ferris et al. 1998). In rice, exposure to a high maximum temperature (>35°C) episodes near flowering can result in a reduction in pollination (Satake and Yoshida 1978; Matsui and Horie 1992); and therefore rice yield is vulnerable to extreme high temperatures during flowering.

In GLAM, the impact of high temperature on wheat flowers has been parameterized and assessed by Li et al. (2010a). This subroutine was modified to simulate the effect of low and high temperate stress on rice, based on previous experiments and ORYZA2000. Equations 2.16–2.18 are the same as those used in ORYZA2000 (Bouman et al. 2001). During flowering, the grain-set fraction of rice decreases when the daily maximum temperature (T_{max}) is above a critical value. Consequently, the rate of change of the harvest index is reduced when the grain-set fraction is below a critical value, resulting in a reduction in the harvest index potential grain yield. The effect of high temperature stress on the fraction of rice fertile spikelets (S_h) is estimated by the follow equation:

$$S_h = 1/ (1 + \exp (0.853(T_{max} - 36.6))) \quad (2.18)$$

The rate of change of the harvest index is also reduced when the fraction of the rice spikelet is lower than a critical value, leading to a reduction in the harvest index and the potential grain yield. The relationship between the harvest index and the fraction of rice spikelet is estimated by the following equation:

$$\frac{\partial H_I}{\partial t} = \left(\frac{\partial H_I}{\partial t}\right)_0 \left(\frac{1 - P_{cr} - MIN(S_c, S_h)}{P_{cr}}\right) \text{For MIN } (S_c, S_h) < P_{cr} \quad (2.19)$$

where $\frac{\partial H_I}{\partial t}$ is the rate of increase in the harvest index. When the grain set fraction is below a critical fractional grain-set P_{cr}, the non-stressed value of the rate of increase in the harvest index $\left(\frac{\partial H_I}{\partial t}\right)_0$ is reduced. The value of P_{cr} is in the range of 0.6–0.8.

2.3 Weather data

The climate variables required to drive the GLAM-Rice are daily minimum/maximum temperature, rainfall, and solar radiation. The weather data used in the GLAM-Rice in this study are historical weather data and the APEC Climate Center Multi-Model Ensemble (APCC MME) seasonal forecast. The daily minimum/maximum temperatures and precipitation at 60 meteorological stations for 1973–2010 were provided by the Korea Meteorological Administration (KMA), and these data were interpolated to regular grid cells at a resolution of $0.25^{o} \times 0.25^{o}$ using the nearest neighbor interpolation method (also known as proximal interpolation or point sampling in some contexts), which is a simple method of multivariate interpolation in 1 or more dimensions (Rukundo and Cao 2012), where the nearest neighbor algorithm simply selects the value of the nearest point. Although the method cannot produce a new value, the value in the new raster is selected by replicating the value of the nearest cell at the shortest distance.

Table 1. Summary of historical climate variables and seasonal forecasts used in the GLAM-Rice.

	Source	Original scale	Rescaling	Periods
Crop data				
Paddy rice yield	Korean statistical database	County	Converted to 0.25° × 0.25° by ArcGIS	1996–2010
Distribution of rice areas	Monfreda et al. 2008	5 min	Aggregated to 0.25° × 0.25°	2000
Soil data				
Soil texture types	FAO digital soil map of the world (Batjes 1997)		Aggregated to 0.25° × 0.25°	
Historical weather data				
Maximum/ minimum temperature	KMA	Daily, meteorological stations	Interpolated to the 0.25° × 0.25° resolution using the nearest neighbor interpolation method	1996–2010
Solar radiation	42 stations estimated by sunshine duration	Daily, meteorological stations		1996–2010
	18 stations measured from KMA			1996–2008
	ERA-interim	Daily, 0.44°×0.44°	Converted to 0.25° × 0.25°	
Rainfall	PRIDE	Daily, 1km×1km	Aggregated to 0.25° × 0.25°	2000–2010
	APHRODITE	Daily,0.25°×0.25°	NO	1996–1999
Maximum/ minimum temperature	PRIDE	Daily, 1km×1km	Aggregated to 0.25° × 0.25°	2000–2010
APCC MME seasonal forecast				
Mean temperature	APCC MME seasonal forecast	Monthly, 2.5°×2.5°	Downscaled to daily data at 57 stations, finally interpolated to 0.25° × 0.25°	1983–2005
Rainfall	APCC MME seasonal forecast	Monthly, 2.5°×2.5°		

Korean statistical database (http://kosis.kr).

Monfreda et al. 2008: http://www.geog.mcgill.ca/~nramankutty/Datasets/Datasets.html

PRIDE: the PRISM based Downscaling Estimation (PRIDE) from KMA.

APHRODITE: Asian precipitation products created by the Research Institute for Humanity and Nature and Meteorological Research Institute of Japan Meteorological Agency (http://www.chikyu.ac.jp/precip/)

In South Korea, the density of meteorological stations is approximately one every 10 km, and this high density allows interpolation of climate variables at these meteorological stations at a resolution of $0.25^{o} \times 0.25^{o}$. The historical daily precipitation from 2000 to 2010 at a 1km × 1km resolution was obtained from KMA, which was interpolated from the station weather data using PRIDE by KMA. The daily precipitation from 2000 to 2010 at a resolution of 1km × 1km was aggregated to $0.25^{o} \times 0.25^{o}$ using the software CDO (Climate Data Operator). The daily precipitation for 1996–1999 is not available from PRIDE, so daily precipitation at the $0.25^{o} \times 0.25^{o}$ resolution from APHRODITE is therefore used instead. Historical daily solar radiation was estimated using the regression equation between global radiation and sunshine duration. A summary of the data sources used for calibrating and validating the forecasting model is shown in Table 1.

For estimating solar radiation, a modified form of the Angstron-type regression equation between global radiation and sunshine hours is generally used, and is thus used in this study to estimate the station solar radiation in South Korea from 1996–2010. Global radiation is estimated using the following equation (from Duffie and Beckman 1994):

$$\frac{\overline{H}}{H_0} = a + b\frac{\bar{s}}{s_0} \tag{2.20}$$

where $\overline{H}$ is the daily global radiation on a horizontal surface ($MJm^{-2}\ day^{-1}$); H_0 is the daily extraterrestrial radiation on a horizontal surface ($MJm^{-2}\ day^{-1}$); $\overline{S}$ is the number of hours of bright sunshine; S is the daily maximum number of hours of possible sunshine (or day length); and a and b are regression constants to be determined. The extraterrestrial solar radiation H_0 on a horizontal surface was calculated from the following equation:

$$H_0 = \frac{24 \times 3.6 \times 10^{-3} \times I_{SC}}{\pi}\left(1 + 0.033\cos\left(360\frac{\overline{D}}{365}\right)\right)\cos\emptyset\cos\delta\sin\omega + \omega\sin\emptyset\sin\delta \tag{2.21}$$

where $I_{SC} = 1367 Wm^{-2}$ is the solar constant, $\overline{D}$ is the Julian day number, $\emptyset$ is the latitude of the location, ω is the sunset hour angle, δ is the declination angle given as:

$$\delta = 23.45\sin\left(360\,\frac{248 + \overline{D}}{365}\right) \tag{2.22}$$

and ω is the sunset hour angle given as:

$$\omega = \cos^{-1}(-\tan\emptyset\tan\delta) \tag{2.23}$$

In addition, the maximum possible sunshine duration $\overline{S_0}$ is given by:

$$\overline{S_0} = \frac{2}{15}\omega \tag{2.24}$$

At stations where there is no data for observed solar radiation, the estimated solar radiation is used. Therefore, the observed solar radiation from 18 stations, and the estimated solar radiation at 42 stations from 1980–2010 in South Korea were interpolated to a $0.25^o \times 0.25^o$ resolution using the nearest neighbor interpolation method. In order to assess how the accuracy of the solar radiation used affected the performance of the skill of the rice forecast, the GLAM-Rice model was run with both the estimated solar radiation and the solar radiation from ERA-Interim at a resolution of $0.25^o \times 0.25^o$ from 1996–2008 in South Korea.

The historical daily precipitation and maximum and minimum temperature at a 1km × 1km resolution, interpolated from the station weather data using PRIDE from KMA, were aggregated to a resolution of $0.25^o \times 0.25^o$ using the software CDO (Climate Data Operator), in order to make a comparison with the nearest neighbor interpolated climate variables. To estimate how the accuracy of temperature affected the performance of the GLAM-Rice in rice yield forecasting, the model was run with the nearest neighbor interpolated temperature and the PRIDE downscaled temperature from 2000 to 2010, respectively.

The seasonal forecasts used for this study were provided by the APEC Climate Center, and include a three-month seasonal forecast (with a lead time of three months) from ten GCMs, and a six-month seasonal forecast (with a lead time of six months) from six GCMs (Table 2). All the models used produced ensemble seasonal hindcasts (i.e. forecasts of past years) from 1983–2005 at a resolution of $2.5^o \times 2.5^o$ on a global scale, and this therefore provided an opportunity to explore crop yield predictability and to perform early crop yield assessments using a crop growth model.

Table 2. Summary of APCC MME seasonal forecasts used in this study

Model	Institution	Ensemble number (ensembles)	Lead Time (months)
CWB	Central Weather Bureau (Taipei)		3
GDAPS_F	Korea Meteorological Administration (Korea)	20	3
HMC	Hydrometeorological Centre of Russia (Russia)	10	3
MSC_CANCM3	Meteorological Service of Canada (Canada)	10	3, 6
MSC_CANCM4	Meteorological Service of Canada (Canada)	10	3, 6
NASA	National Aeronautics and Space Administration (USA)	11	3, 6
NCEP	Climate Prediction Center / NCEP/NWS/ NOAA (USA)	20	3, 6
PNU	Pusan National University (Korea)	15	3, 6
POAMA	Centre for Australian Weather and Climate Research/ Bureau of Meteorology (Australia)	30	3, 6
SCM		MME	3

As there is a mismatch between the spatial and temporal scales of the seasonal forecast dataset and the input requirements of the crop model, the monthly mean temperature and monthly rainfall at a resolution of $2.5^{o} \times 2.5^{o}$ were spatially and temporally downscaled to the daily maximum and minimum temperature and rainfall at a finer surface resolution. Firstly, the monthly rainfall and mean temperature at 57 stations in South Korea was abstracted from the APCC MME dataset. The bias correction was made by adding the anomalies of monthly temperature (the difference between the predicted value and the predicted average value for the period 1983–2005) to the monthly averaged value of observations, as in Eq. 2.25 below. For precipitation, if the value of the difference was negative, the anomalies were corrected as the ratio between the predicted values and the observation, as in Eq. 2.26:

$$T'_{y,m} = (T_{y,m} - T_{83\_05,m}) + CRU\_T_{83\_05,m} \quad (2.25)$$

$$P'_{y,m} = \begin{cases} (P_{y,m} - P_{83\_05,m}) + CRU\_P_{83\_05,m} & P_{y,m} \geq P_{83\_05,m} \\ \left(\frac{P_{y,m}}{P_{83\_05,m}}\right) \times CRU_{P\,83\_05,m} & P_{y,m} < P_{83\_05,m} \end{cases} \quad (2.26)$$

where T is temperature, P is precipitation, y is year, and m is month, representing the past periods of observation and forecast data.

In addition to the spatial downscaling of rainfall and temperature from APCC MME at a resolution of 2.5° × 2.5° for 57 meteorological stations, the temporal downscaling of APCC MME from monthly to daily was also required to serve as input to the crop model. The bias corrected monthly average precipitation and average temperature (2-m air temperature) data at 57 meteorological stations were then compared with those of the observations, in order to select the best forecast data from the available historical data for a specific year/month. The procedures involved in temporal downscaling were as follows. Firstly, the average value of the prediction from the bias corrected forecast data was calculated at 57 meteorological stations. Secondly, the average of the monthly observations from 57 stations for 36 years was similarly calculated, and then the difference between the average of the forecast data and the average of the past observations was calculated using two variables (precipitation and average temperature). Thirdly, when the smallest distance was evident between the average of the monthly observations and that of the forecast data, the historical daily observation data were then selected as the daily forecast data. Finally, a specific year/month (best fit month) was then forecast from 57 meteorological stations from the date of the selected data. If there was a large difference between the prediction and the observation, bias correction was conducted using the methods described above.

2.4 Crop and soil dataset

South Korea is the study region, and the study period is 1996 to 2010; during this period, both input weather and observed paddy rice yield data are available. Last year the GLAM-Rice was validated at the provincial level of South Korea (Li 2013). In addition, the historical county-level paddy rice yield from 1996–2010 in South Korea was recently obtained from the Korean statistical database (http://kosis.kr). This therefore enables us to estimate the goodness of fit of the model on a smaller scale. Lowland rice is usually irrigated, and it is therefore not very sensitive to changes in rainfall, but it does depend on adequate solar

radiation and temperatures. To match the gridded weather data, rice yields at the county level were aggregated into a 0.25° × 0.25° resolution by ArcGIS using an area-weighted mean. This dataset was then used to calibrate and validate the performance of the GLAM-Rice in South Korea.

The dominant agricultural soil texture types were obtained from the FAO digital soil map of the world (Batjes 1997), and were then aggregated to the 0.25° × 0.25° resolution using the area-weighted mean by ArcGIS. The rice planting date, and the days between planting and harvest were estimated according to global crop calendar maps for 19 crops (from Sacks et al. 2010). These datasets include gridded maps of planting dates, harvesting dates, and growing seasons at 5 min × 5 min and 0.5° × 0.5° resolutions, and were obtained by digitizing and georeferencing existing observations of crop planting and harvesting dates. An observation is included in every grid if the observed crop calendar is available for each region. The geographic distribution of rice areas for South Korea (Figure 5) was then abstracted from the global map of Harvested Area and Yields of 175 crops by Monfreda et al. (2008), which includes the NetCDF and ArcGIS ASCII format dataset at a resolution of 5 min × 5 min. This map is used to determine which grid cells contain rice, and if there is no rice in a particular grid cell then the GLAM skips that particular cell. These datasets were produced by integrating the national, state, and county level census statistics with a recently updated global data set of croplands at a 5 min × 5 min (about 10 km × 10 km) resolution. As shown by Figure 5, rice is mainly cultivated in the west, southwest, and southeast part of South Korea, while only limited amounts of rice are planted in the northern part of South Korea because the area is mountainous.

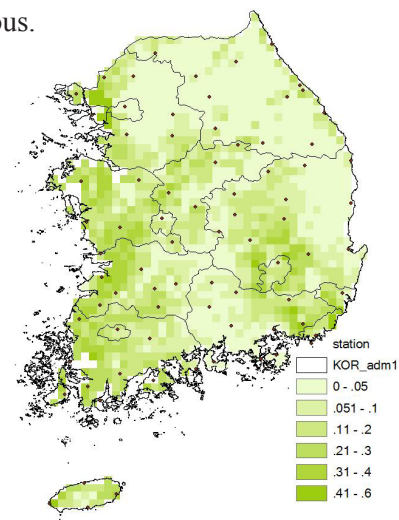

Figure 5. Map showing areas where rice is harvested in South Korea, as a proportion of each grid cell.

2.5 Relationship between the input dataset and the model's skill

In order to estimate how the accuracy of solar radiation data affects the forecast skill of the crop model, the GLAM-Rice was run using solar radiation data from ERA-Interim and solar radiation interpolated from station data using the nearest neighbor interpolation method, on a resolution of 0.25° × 0.25° from 1996 to 2010 over South Korea. The 0.25° × 0.25° resolution rainfall was obtained from APHRODITE for 1996–1999 and from PRIDE for 2000–2010 (Table 1). The 0.25° × 0.25° resolution rainfall from PRIDE was obtained by aggregating 1 km × 1 km resolution rainfall using the area-weighted average. The daily maximum/minimum temperature at a resolution of 0.25° × 0.25° was interpolated from meteorological stations using the nearest neighbor interpolation method.

In order to examine how the accuracy of temperature affects the performance of the crop model, the GLAM-Rice was driven using the nearest neighbor interpolated temperature and PRIDE downscaled temperature at a resolution of 0.25° × 0.25° from 1996 to 2010 in South Korea, respectively. The 0.25° × 0.25° resolution rainfall was obtained from APHRODITE for 1996–1999, and from PRIDE for 2000–2010 (Table 1). The daily maximum/minimum temperature and solar radiation at a resolution of 0.25° × 0.25° was obtained using the nearest neighbor interpolated temperature and solar radiation.

To find the appropriate spatial scale of climate variables for use in running the crop model, the GLAM-Rice was driven by the 0.25° × 0.25°, 0.5° × 0.5°, and 1° × 1° resolution climate variables from 1996 to 2010 over South Korea. The 0.25° × 0.25° resolution rainfall was obtained from APHRODITE for 1996–1999 and from PRIDE for 2000–2010. The daily maximum/minimum temperature and solar radiation at a resolution of 0.25° × 0.25° was obtained from the nearest neighbor interpolated temperature and solar radiation, and the 0.5° × 0.5° and 1° × 1° resolution weather data were obtained by aggregating the 0.25° × 0.25°resolution weather data.

In order to assess how the temporal scale of climate data affects the forecast ability of the crop model, the GLAM was driven by daily climate variables and 30 days average rainfall, temperature, and solar radiation, at the representative sites in South Korea. Three sets of experiments were conducted. In the first set of experiments, the GLAM-Rice was run with the daily maximum and minimum temperatures, solar radiation, and the 30 day averaged rainfall. In the second set of experiments, daily rainfall and solar radiation (averaged over

30 days) were applied over the maximum and minimum temperatures. In the third set of experiments, daily rainfall and maximum and minimum temperatures were used, while solar radiation (averaged over 30 days) was applied.

2.6 Hindcast methodology

The GLAM-Rice was used to simulate paddy rice yields using observed weather data and downscaled APCC MME hindcast data, with the ensemble mean of each single GCM (the average of the ensemble members in each GCM), and the multi-model ensemble mean provided by the APEC Climate Center. The flowchart of the regional weather/crop forecasting system is shown in Figure 6. Firstly, the APCC MME monthly seasonal forecast at a resolution of $2.5^{o} \times 2.5^{o}$ from 1983–2005 was spatially and temporally downscaled to daily climate variables at 57 meteorological stations (Section 2.3), and this was interpolated to regular grid cells at a resolution of $0.25^{o} \times 0.25^{o}$ using the nearest neighbor interpolation method. (The downscaled weather forecast was then linked with the crop model to determine the spatial/temporal working scale and spatial parameters). Finally, the model output and hindcast rice yield were processed. Three sets of hindcasts were carried out using the GLAM-Rice. In the first experiment, the crop model was run using the observed weather data alone, which was used as a reference to compare and evaluate the performance of APCC MME hindcast. The second set of hindcasts then used the ensemble mean of each single GCM to drive the GLAM-Rice; and the third set of simulations used the ensemble mean of multi-models to drive the crop model. For the second and third sets simulations, the APCC MME hindcasts were updated with observations using the progression of seasons, to test if updating seasonal forecasts would improve the forecast skill. In doing so, the crop growth simulations were driven by observations up to a certain date, and were then driven by the downscaled APCC MME hindcasts up to the date of rice harvest.

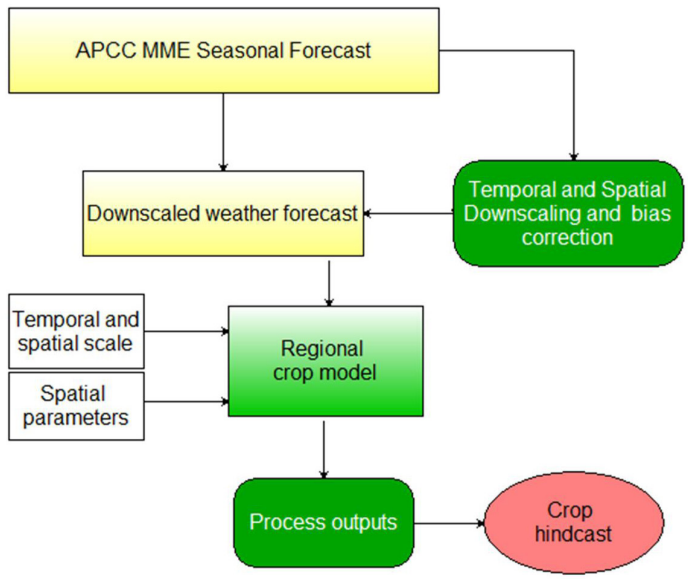

Figure 6. Flowchart of the regional crop forecasting system. The spatial downscaling of rainfall and temperature is from APCC MME at a resolution of 2.5° × 2.5° from 57 meteorological stations; temporal downscaling of MME uses monthly to daily data (see Section 2.3).

For the six months seasonal forecast, four simulations were conducted for each set of hindcast in order to predict rice during the growth season encompassing May, June, July and August. Observed weather data were used for simulations up to 30 April, 31 May, 30 June, and 31 July, respectively. From the latter dates onwards, the model was run using the downscaled ensemble mean of each single GCM. The simulation results were later spatially aggregated to a national level for validation and prediction skill of crop yield. In addition, the simulated rice yield from aggregation was later compared with statistical national rice yields to test if the GLAM-Rice and the APCC MME seasonal forecasts could be used for predicting rice yield. Furthermore, predicted yields using APCC MME hindcasts were compared to observed paddy rice yield and the simulated yield obtained by forcing the crop model with observed climate variables, in terms of the correlation coefficient between the observed and simulated yield and the RMSE, which represents a mean weighted difference (mean distance) between predicted and observed data.

We use the Pearson's coefficient of linear correlation to measure the goodness-of-fit of the model, and to evaluate the accuracy of the rice yield predictions. The correlation

coefficient is expressed as the following equation:

$$r = \frac{\sum_{i=1}^{n}(X_i - \overline{X})(Y_i - \overline{Y})}{\sqrt{\sum_{i=1}^{n}(X_i - \overline{X})^2}\sqrt{\sum_{i=1}^{n}(Y_i - \overline{Y})^2}} \tag{2.27}$$

where r is the correlation coefficient between the observed and predicted crop yield, n is number of years i, X_i and Y_i are observed and predicted yield, respectively, and $\overline{X}$ and $\overline{Y}$ are observed and predicted average yield, respectively.

We use the RMSE between the predicted and observed yield to evaluate the error of the rice yield prediction. The root-mean-squared error of prediction is:

$$RMSE = \sqrt{\frac{\sum_{i=1}^{n}(X_i - Y_i)^2}{n}} \tag{2.28}$$

where *RMSE* represents the overall error weighted by the square of deviations, n is the number of years, i; and X_i and Y_i are the observed and predicted yields, respectively.

Two sets of calibration methods were used to assess how particular calibration methods affect the forecast skill of the GLAM-Rice model. In the first method, a single pair of yield yap parameters was calibrated by driving the crop model using the multi-model ensemble mean. In the second method, the ensemble mean of each single GCM was used to calibrate a pair of yield yap parameter values for each GCM. It was considered that the second calibration would possibly be able to partially correct the bias of each individual GCM, because the optimal value of yield yap parameters at each grid cell was obtained by minimizing the root mean square error between observed and simulated yield.

Both dependent and independent calibration was carried out to test whether calibration should be conducted using the yield from the current period or from previous periods. For dependent validation, the GLAM-Rice was run using the calibrated yield yap parameters for two time periods 1996–2000 and 2001–2005, respectively. For 1996–2000, rice yield was predicted using the calibrated YGP for 1996–2000, and similarly the calibrated YGP for 2001–2005 was used to predict rice yield for 2001–2005. For cross-validation, the calibrated YGP for 1996–2000 was used to predict rice yield for 2001–2005, and vice versa. By calibrating the YGP, the mean yield can be bias corrected, therefore making the predicted mean yield much closer to the observed mean yield. However, calibration of the

YGP cannot affect the variability of the yield, and the variability of the yield is determined by the skill of the GLAM-Rice.

To compare the performance of the multi-model yield ensemble mean with that of the individual models, a further forecast was conducted by driving the crop model using multi-model ensemble mean weather variables and the ensemble mean of each single GCM. Driving the GLAM-Rice by the multi-model ensemble mean, and averaging the output of GLAM forced by the ensemble mean of each single GCM was carried out for the multi-model ensemble mean forecast to examine which skills were able to improve the forecast skill of the crop model.

For a three-month seasonal forecast, two simulations were conducted for each set of hindcast in order to predict the rice yield in the middle of the rice growth season (August). In the first experiment, three months seasonal forecast was used up to July 31. In the second case, observed weather data were used for simulations up to 31 July. For both experiments, after July 31 the model was run with the downscaled multi-model ensemble mean of each single GCM. The simulation results were then spatially aggregated to a national level for validation and prediction of crop yield.

2.7 Satellite-derived Land Use and Leaf Area Index (LAI)

The level-4 combined (Terra and Aqua) MODIS provides a global LAI every 8 days at a resolution of 1 km × 1 km (https://lpdaac.usgs.gov/products/modis_products_table/mcd15a3). However, the MODIS LAI is discontinuous and incoherent on a temporal and spatial scale, due to the effect of cloud and seasonal snow cover, and there are limitations in the instrument and retrieval algorithm, which affect application in land surface modeling (Yuan et al. 2011). Improved MODIS LAI products were generated by Yuan et al. (2011) using both a temporal spatial filter and the Savitzaky-Golay filter, and the resultant MODIS LAI product provides results every 8 days at a resolution of 1 km × 1 km on a global scale from 2000 to 2009 via the Land-Atmosphere Interaction Research Group at Beijing Normal University. These LAI products include the LAI of all vegetation on the surface of the land. To abstract the LAI for rice, a land use map of paddy fields was abstracted from the Global Land Cover by National Mapping Organizations (GLCNMO) at a resolution of 1 km × 1 km (30 arc seconds), including 20 land cover items that were created using MODIS data observed in 2003 (TERRA Satellite) (http://www.iscgm.org/gmd/download/

glcnmo.html). The improved MODIS LAI for rice of South Korea provides results every 8 days at a resolution of 1km × 1km (Figure 7), and it was abstracted based on the land use map of the paddy field described above. The 8 days improved MODIS LAI for rice was linearly interpolated into a daily value to match the input requirement of the crop model. Finally, the daily improved MODIS LAI at a resolution of 1 km × 1 km in South Korea was integrated into a resolution of $0.25^{o} \times 0.25^{o}$, and used to replace the original LAI in the GLAM-Rice.

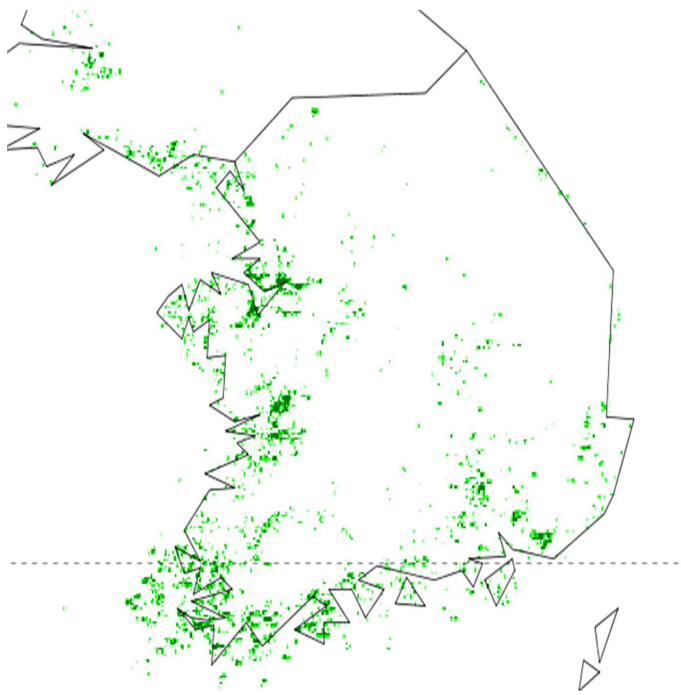

Figure 7. Abstracted land use map of paddy fields of South Korea, obtained from the Global Land Cover by National Mapping Organizations (GLCNMO) at a resolution of 1km × 1km (30 arc seconds) in 2003 (TERRA Satellite).

3. RESEARCH RESULTS

3.1 The effect of input data accuracy on forecast skill

3.1.1 Solar radiation

Most lowland rice is irrigated, and therefore the prediction accuracy of the lowland rice yield is not very sensitivity to changes in rainfall, but does depend on the accuracy of solar radiation and temperature. The averaged seasonal total solar radiation from 2000 to 2010 in South Korea was in the range of 2015 to 3000 MJ/m^2, with small spatial variations (Figure 8). Relatively low solar radiation can be found in some of the grid cells in the north part of South Korea, which are not major rice planting regions. To determine which climate factors influence the inter-annual variation of paddy rice yield in South Korea, the correlations between rice yield anomalies and anomalies of seasonal mean temperature and seasonal total solar radiation at a national level for 1996–2010 were analyzed using the Pearson correlation. The yield anomalies, temperature anomalies, and solar radiation anomalies were obtained by removing linear trends in yield, temperature, and solar radiation from yield, temperature, and solar radiation, respectively. For the years 1996–2010, a weak correlation ($r = 0.357$, $p = 0.19$) between rice yield anomalies and temperature anomalies was found; however, there was a significant correlation ($r = 0.62$, $p < 0.05$) between rice yield anomalies and intercepted solar radiation anomalies (Figure 9). To further examine how each climate variable affects the rice yield, the rice yield was regressed against the climatic variables (mean growing season temperature and total growing season intercepted solar radiation) for 1996–2000, using the multiple linear regression method, which showed that R^2 values made independent contributions to each climate variable in relation to the variability of rice yield. The intercepted solar radiation, temperature, and the interaction between the intercepted solar radiation and temperature, determined about 42%, 16% and 17% of variability in rice yield from 1996 to 2010, respectively. However, although about 25% of variability in the rice yield was affected by other factors, the inter-annual variability of rice yield can be largely explained by the intercepted solar radiation. This indicates that in South Korea, solar radiation was one of the important climate variables affecting the interannual variability of paddy rice yield from 1996 to 2010.

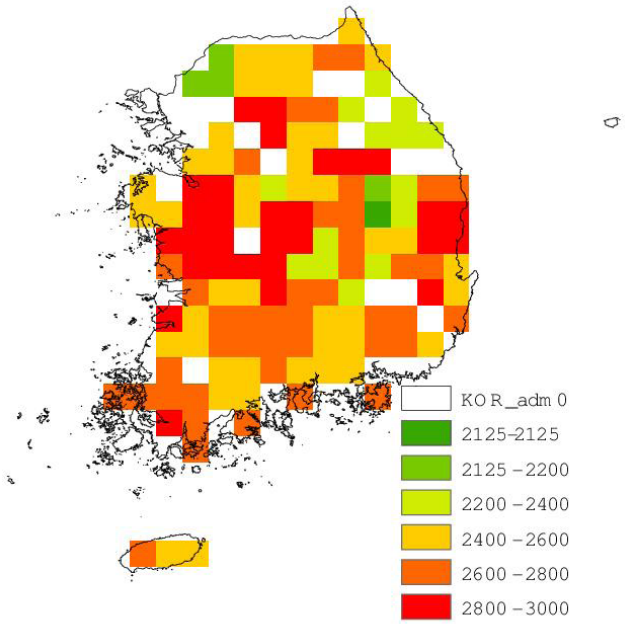

Figure 8. Average values of seasonal total solar radiation (MJ/m^2) in South Korea from 2000 to 2010

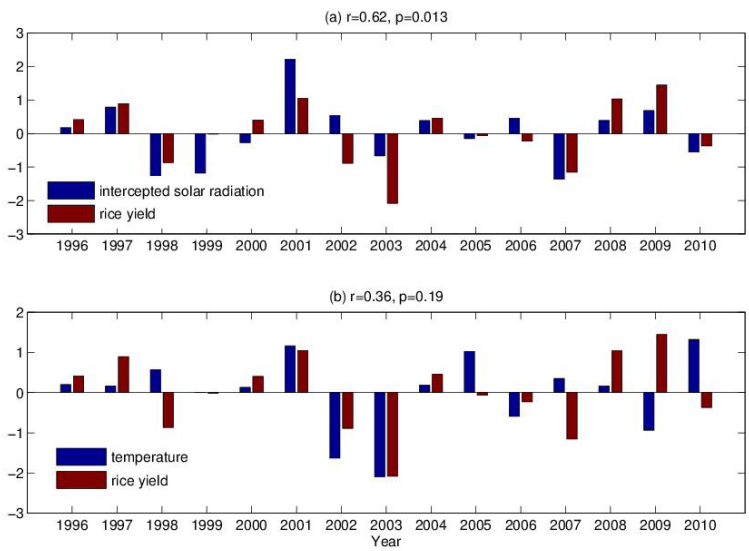

Figure 9. (a) Correlation coefficient between rice yield anomalies and intercepted solar radiation anomalies at the national level of South Korea, from 1996 to 2010; (b) correlation between rice yield anomalies and temperature anomalies at the national level of South Korea, from 1996 to 2010.

To evaluate the performance of the modified form of the Angstron-type regression equation in estimating solar radiation, a comparison of the estimated daily solar radiation and the measured daily solar radiation at 18 meteorological stations in South Korea is shown in Table 3. In general, the modified form of the Angstron-type regression equation led to reasonable estimations of daily solar radiation. The coefficient of determination, R^2, between the estimated and measured daily solar radiation at 18 meteorological stations varied from 0.68 for Suwon, to 0.816 for Jeju between 1985 and 2010 (Figure 10). The estimated solar radiation explains at least 68% of the variability in measured solar radiation. In all locations, daily solar radiation predicted by the Angstron-type regression equation was in close agreement with that obtained from meteorological stations, despite overestimations of solar radiation on some days (Figure 10). It is therefore considered that the Angstron-type regression equation could be used to estimate daily solar radiation at selected research sites, and possibly in other places with similar climatic conditions.

Table 3. Comparison of estimated daily solar radiation (MJ m^{-2} day^{-1}) with measured daily solar radiation (MJ m^{-2} day^{-1}) at 18 meteorological stations in South Korea, from 1985 to 2010; R^2 is the coefficient of determination between the estimated and measured daily solar radiation

Location	R^2	Slope	Intercept
Daegwallyeong	0.711	0.902	0.532
Chuncheon	0.749	1.003	-0.449
Gangneung	0.730	0.974	-0.279
Seoul	0.684	0.968	0.617
Incheon	0.712	1.011	0.093
Wonju	0.736	0.963	-0.426
Suwon	0.68	0.998	0.378
Seosan	0.744	1.02	-0.826
Cheongju	0.725	1.018	-0.262
Daejeon	0.725	0.988	-0.305
Chupungnyeong	0.70	0.98	0.454
Andong	0.71	0.998	-0.136
Pohang	0.727	0.981	-0.106
Daegu	0.723	1.00	-0.624
Busan	0.692	0.977	0.6203
Mokpo	0.772	1.00	-0.96
Jeju	0.816	1.016	-0.0302
Jinju	0.736	0.954	-0.449

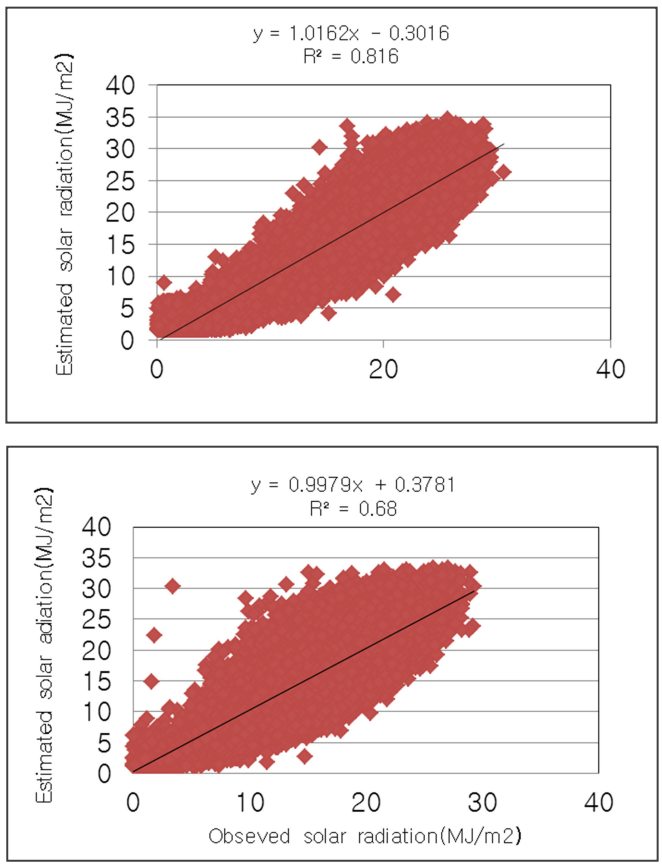

Figure 10. A comparison of estimated daily solar radiation and measured solar radiation at Jeju (top) and Suwon (bottom) from 1985 to 2010.

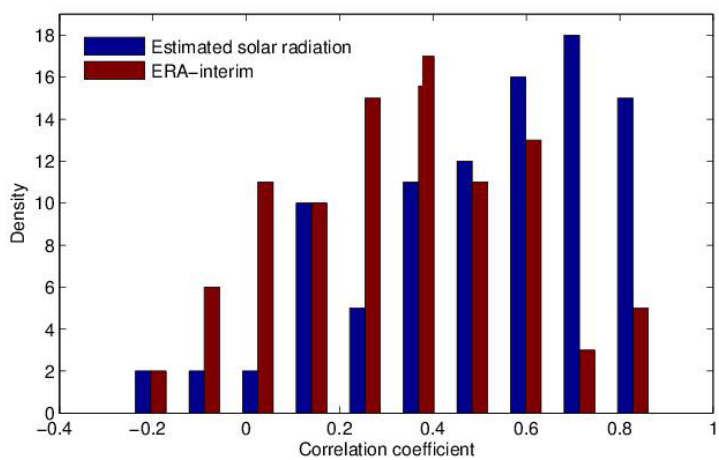

Figure 11. Comparison of correlation between observed and simulated rice yield at a resolution of 0.25° × 0.25°, when the GLAM-Rice was run using estimated solar radiation and solar radiation from ERA-interim for 1996–2008, respectively

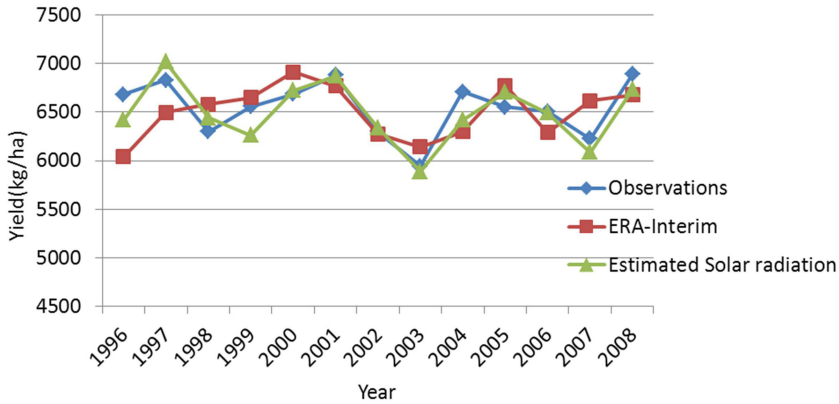

Figure 12. Comparison of observed and simulated rice yield at the national level of South Korea, where GLAM-Rice was run with estimated solar radiation and solar radiation from ERA-interim for 1996–2008, respectively

In order to assess how the accuracy of the solar radiation product affects the performance of the yield prediction, the GLAM-Rice model was run with the estimated solar radiation and solar radiation from ERA-Interim at a resolution of $0.25^{o} \times 0.25^{o}$ in South Korea, from 1996 to 2008, respectively. The density of the correlation coefficient between the observed and simulated yields is shown in Figure 11. When the GLAM-Rice was driven by the estimated solar radiation, the correlation coefficient between the observed and simulated rice at a resolution of $0.25^{o} \times 0.25^{o}$ was obviously higher than that from solar radiation of ERA-Interim. Similarly at the national level, there was a weak correlation ($r = 0.369$, $p = 0.215$) between the observed and simulated rice yield when driving the model with solar radiation from ERA-interim (Figure 12). The simulated yield was not able to capture the inter-annual variability of observations, and this is considered to be probably related to the fact that ERA-interim cannot adequately reproduce both the temporal and spatial variability of solar radiation. In contrast, there is good agreement at the national level ($r = 0.849$, $p < 0.001$) between the observed and simulated paddy rice yield when driving the crop model using estimated solar radiation (Figure 12). Running the GLAM-Rice with estimated solar radiation greatly improved the skill of the model, both at an individual grid cell and at a national level. This indicates that making improvements in the accuracy of solar radiation is very important for the skill of the paddy field rice yield forecast. Similarly, the experimental results also proved that solar radiation (irradiance) has a substantial influence on the irrigated rice yield, and the yield components issuing from the period of panicle initiation to maturity (Islam and Morison 1992).

3.1.2 Temperature

To evaluate the performance of the GLAM-Rice, the model was firstly run using interpolated temperature and rainfall from PRIDE. Large differences were seen in some locations between the observed and simulated yields (Figure 13a), and these differences are found in particular years for the nearest neighbor interpolated temperature from meteorological stations and temperature from PRIDE (Figure 14). Generally, the PRIDE downscaled temperature is lower than that from the nearest neighbor interpolation, particularly for the low temperature region. The topography of South Korea is inhomogeneous, and approximately 30% of the country's area is covered by lowlands; the remaining areas consist of uplands and mountains. The PRIDE downscaled temperature at a resolution of $0.25^{o} \times 0.25^{o}$ was only able to represent the average temperature for each grid cell. Paddy rice is planted on lowland, and the downscaled temperature from PRIDE at a resolution of $0.25^{o} \times 0.25^{o}$ is not able to represent the temperature in the main rice planting region. This leads to a large underestimation of the rice yield in particular years (Figure 13a) due to the lower temperature, which means that the gridded climate variables on a relatively larger scale, such as temperature, cannot be used to simulate crop yield in regions where there is complex topography. However, as meteorological stations are mostly located in regions with relatively low elevation, temperature obtained from these stations is more close to that of the crop growing regions.

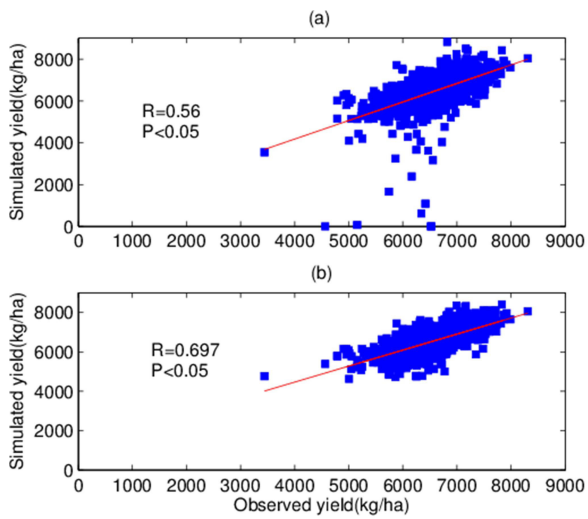

Figure 13. Scatter plot of observed rice yield against simulated rice yield for 2000–2010 at a resolution of $0.25^{o} \times 0.25^{o}$ in the main rice growing region of South Korea, when the GLAM-Rice was run with (a) PRIDE downscaled temperature, and (b) nearest neighbor interpolated temperature.

In order to estimate how the accuracy of temperature data affects the performance of the GLAM-Rice in rice yield forecasting, the model was run using the nearest neighbor interpolated temperature and PRIDE downscaled temperature, respectively. Driving the model with the nearest neighbor interpolated temperature showed a higher forecast skill compared to use of the PRIDE downscaled temperature, both at the individual grid cell (Figure 15) and at the national level of South Korea (Figure 13). This may result from the fact that the nearest neighbor interpolated temperature is much closer to the temperature of the main cropping areas. furthermore, there is either inaccuracy in the PRIDE downscaled temperature, or it not able to represent the real temperature in the main cropping areas, but is able to represent its spatial averages.

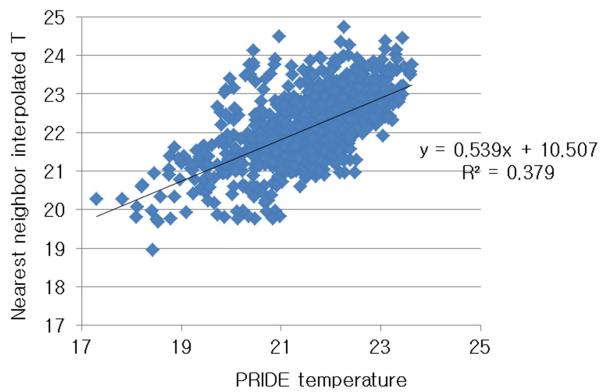

Figure 14. A scatter plot of PRIDE downscaled temperature (℃) against the nearest neighbor interpolated temperature (℃) for 2000–2010 on a resolution of 0.25° × 0.25° in the main rice growing region of South Korea.

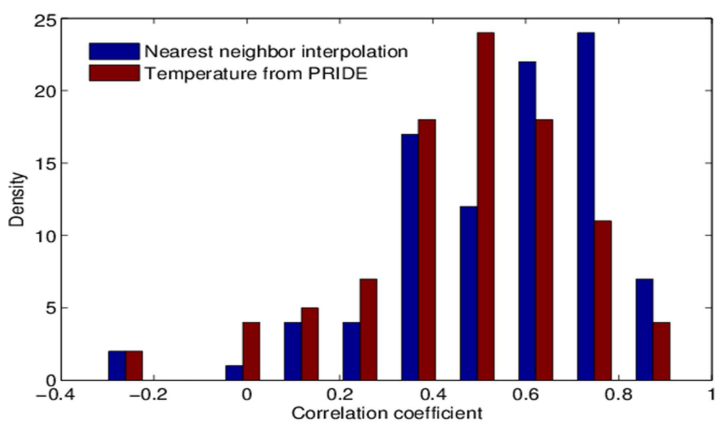

Figure 15. Density of the correlation coefficient between the observed and simulated rice yield for 2000–2010 at a resolution of 0.25° × 0.25° in the main rice growing region of South Korea, when the GLAM-Rice was run with (a) the PRIDE downscaled temperature and (b) the nearest neighbor interpolated temperature.

3.2 Scale of input data

3.2.1 Spatial scale

To illustrate how the spatial scale of climate variables affects the forecast skill of a dynamical regional crop model, the GLAM-Rice was run with the gridded climate data on a small resolution of 0.25°×0.25° and coarser resolutions of 0.5°×0.5° and 1°×1°; the simulated yield at each grid cell was aggregated to the national level of South Korea. The comparison of integrated national yields showed that driving the GLAM using the 0.25° × 0.25° resolution climate data resulted in a higher correlation between the observed and simulated rice yield at a national level (Figure 16). However, when the resolution of the climate data was increased from 1°×1° to resolutions of 0.5°× 0.5° and 0.25° × 0.25°, there was limited improvement in the model's ability to reproduce the interannual variability of the observed yield (Figures 16 and 17). Paddy rice is generally grown under flooded conditions (irrigated conditions), and therefore yield is not very sensitivity to the amount of rainfall, but is sensitive to temperature and solar radiation (as previously mentioned). Furthermore, temperature and solar radiation are smooth variables at a spatial scale, and variability in the spatial scale is relatively small compared to rainfall. Therefore, the forecast skill of the GLAM-Rice is not very sensitive to changes in the spatial scale of climate variables from the smaller 0.25°×0.25° resolution to the coarser 1°×1° resolution. This indicates that it is possible to use the coarser 1° × 1° resolutions to forecast the rice yield for South Korea, and in similar crop environmental regions.

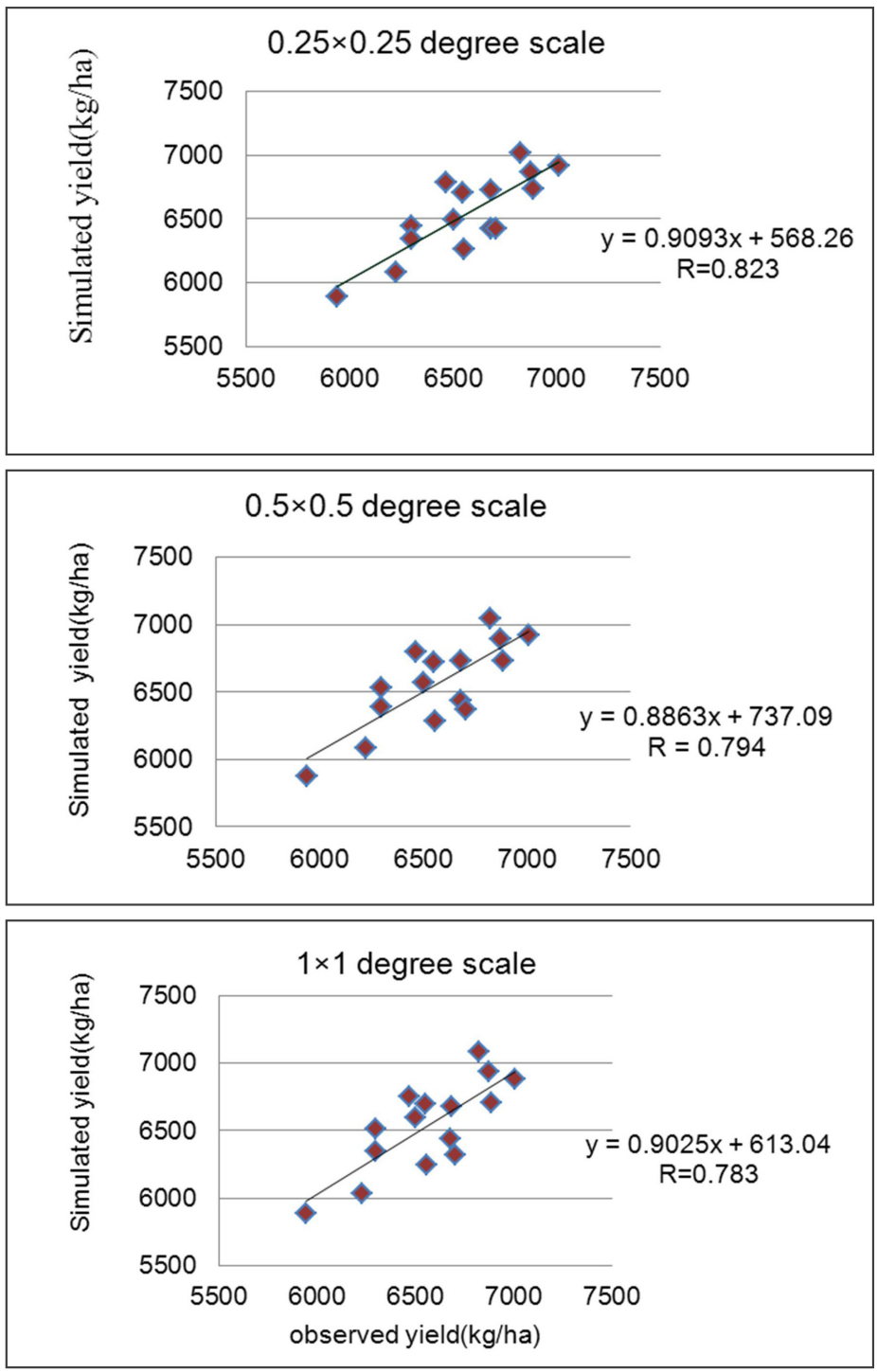

Figure 16. Scatter plot of observed rice yield against simulated rice yield for 1996–2010 in the main rice growing region of South Korea; the GLAM-Rice was run with the 0.25° × 0.25°, 0.5°× 0.5°, and 1°× 1° resolution climate variables.

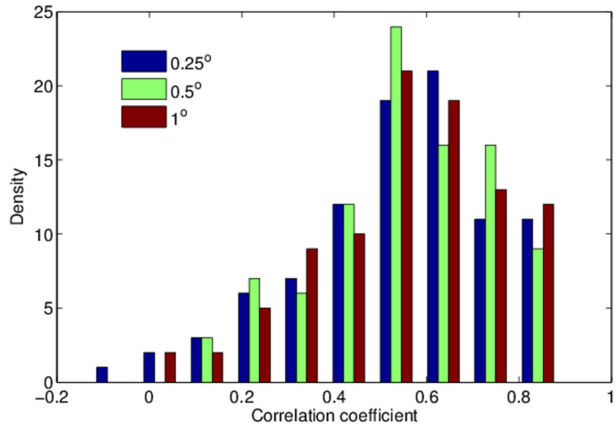

Figure 17. Density of correlation coefficient between observed and simulated rice yield for 1996–2010 in the main rice growing region of South Korea; the GLAM-Rice was run with the 0.25° × 0.25°, 0.5° × 0.5°, and 1° × 1° resolution climate variables.

3.2.2 Temporal scale

In order to demonstrate if the monthly averaged climate variables can be used in a forecast of crop yield, the dynamical crop model was run with the daily and 30-day averaged climate variables respectively. In the first set of experiments, the monthly average rainfall was used when the maximum and minimum temperature and solar radiation were in daily step. Figure 18a shows a comparison of the observed and simulated rice yield when the GLAM was driven by the daily and 30-day average values of rainfall. Results show that using the 30-day average rainfall resulted in a similar yield compared to that using the original daily rainfall for the representative site of South Korea. This indicates that the monthly average rainfall can be used for a forecast of the paddy rice yield for South Korea, because paddy rice is normally irrigated and is not sensitive to the temporal scale of rainfall.

The monthly averaged values of temperature or solar radiation are also used to drive the GLAM-Rice model, respectively. Driving the model with the 30-day average temperature, or with solar radiation, led to a larger difference compared to the predicted yield with daily temperature or daily solar radiation. When using the average temperature or solar radiation over 30 days in GLAM, the yield was evidently overestimated by the model. In addition, when driving the model using monthly temperature or solar radiation it was

unable to capture the yield reduction due to low temperature/solar radiation stress, because when averaged over 30 days the short term variability can be filtered out. In the actual environmental, low temperature/solar radiation stress on a particular day, or in a certain growth stage, can significantly reduce crop yield, and therefore the prediction of rice yield can be significantly affected by the temporal scale of temperature or solar radiation. Therefore, reliable temporal downscaling of monthly temperature and solar radiation to a daily value is required to improve the forecast skill of the regional rice model.

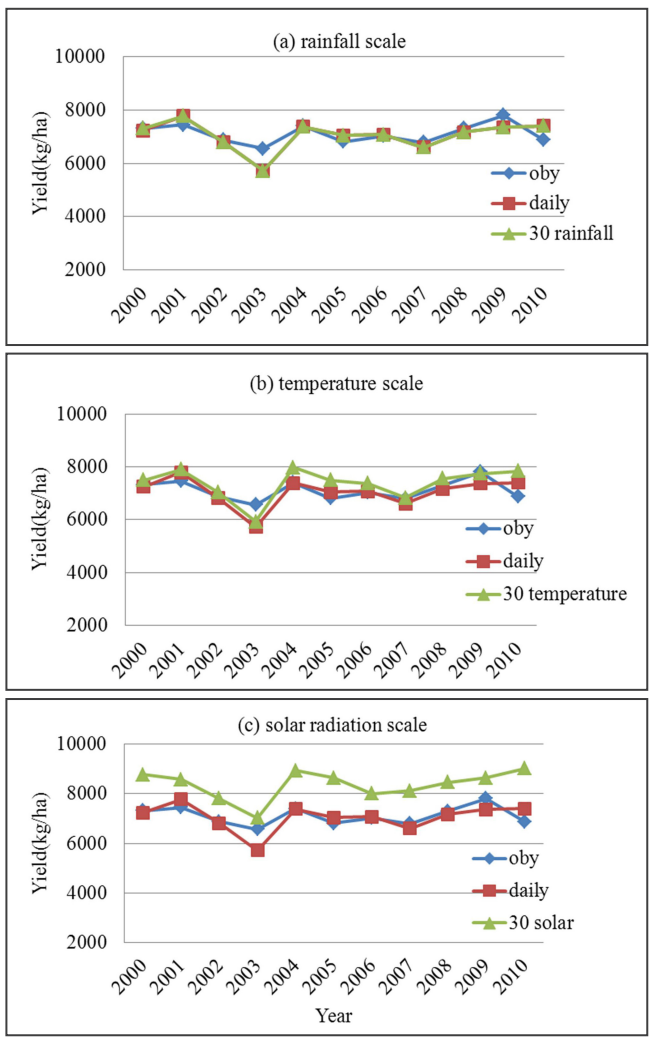

Figure 18. The effect of temporal scale on the skill of the crop model: a) temporal scale of rainfall; b) temporal scale of temperature; c) temporal scale of solar radiation. Abbreviations are as follows: oby: observed rice yield; daily: simulated rice yield by forcing the crop model with daily climate variables; 30 rainfall: simulated rice yield with 30-day averaged rainfall; 30 temperature: simulated rice yield with 30-day averaged temperature; 30 solar: simulated rice yield with 30-day averaged solar radiation.

3.3 Seasonal hindcast of climate and rice yield

3.3.1 Seasonal hindcast of climate

Figure 19 shows the scatter plot of the seasonal forecast of mean temperature from six CGMs against the observed seasonal mean temperature for 1996–2010, at a resolution of $0.25^{o} \times 0.25^{o}$ in the main rice-growing region of South Korea. Temperature from NASA and MSC_CANCM4 show a higher correlation with observations compared to the other single GCMs at the national level of South Korea. However, there is a lower skill in terms of the correlation coefficient for PNU and POAMA. The multi model ensemble mean shows a similar skill to the best single model of NASA. There is no large difference in the forecast skill between each GCM in term of the prediction of seasonal mean temperature. In contrast, none of the GCMs are able to predict the variability of observed seasonal total rainfall (Figure 20), and this was underestimated by the seasonal forecast model. As already mentioned, paddy rice in South Korea is cultivated under irrigated conditions, and therefore rice yield is not sensitive to the amount of rainfall and inaccuracies in predicted rainfall have no significant impact on the forecast skill of the crop model. This indicates that it would not be possible to use the rainfall forecast from these GCMs to predict the seasonal crop yield under rainfed conditions, and a further improvement in the forecast accuracy of rainfall is required to predict the rainfed crop yield.

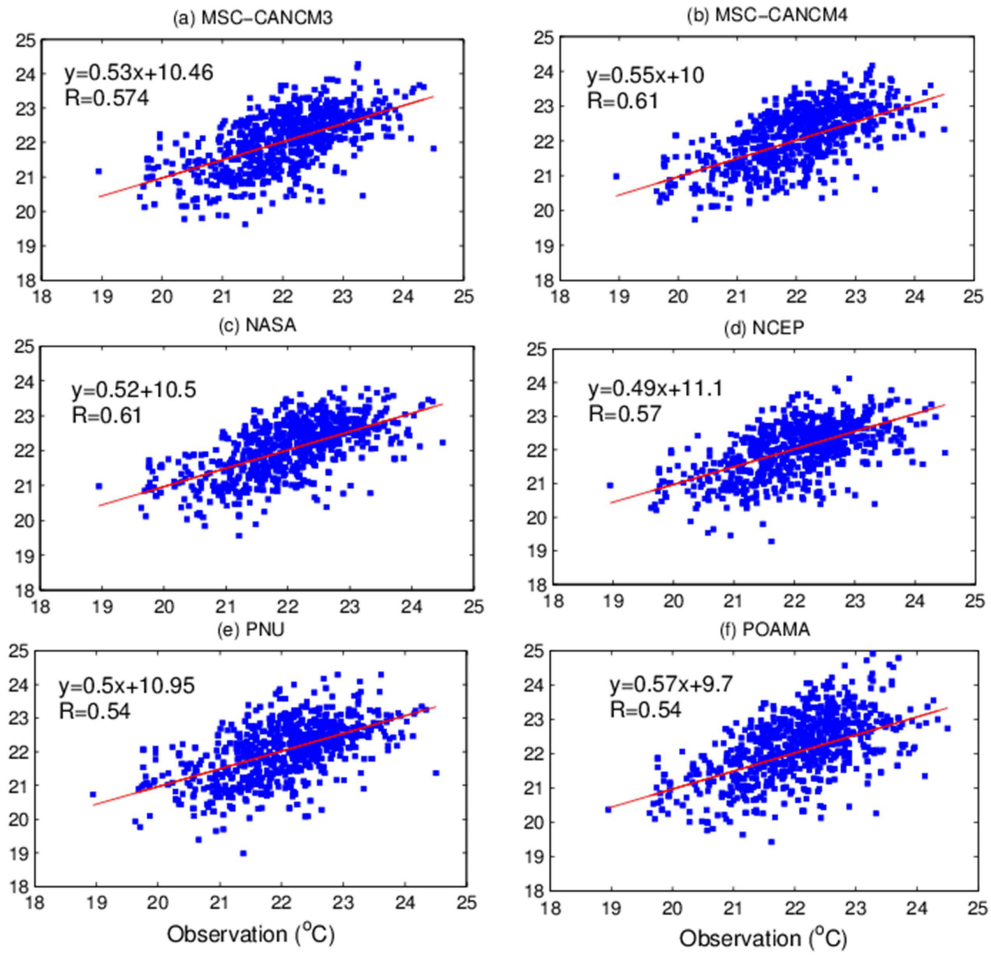

Figure 19. Scatter plot of seasonal mean hindcast temperature data against the observed seasonal mean temperature for 1996–2005, at a resolution of 0.25 × 0.25, in the main rice-growing region of South Korea.

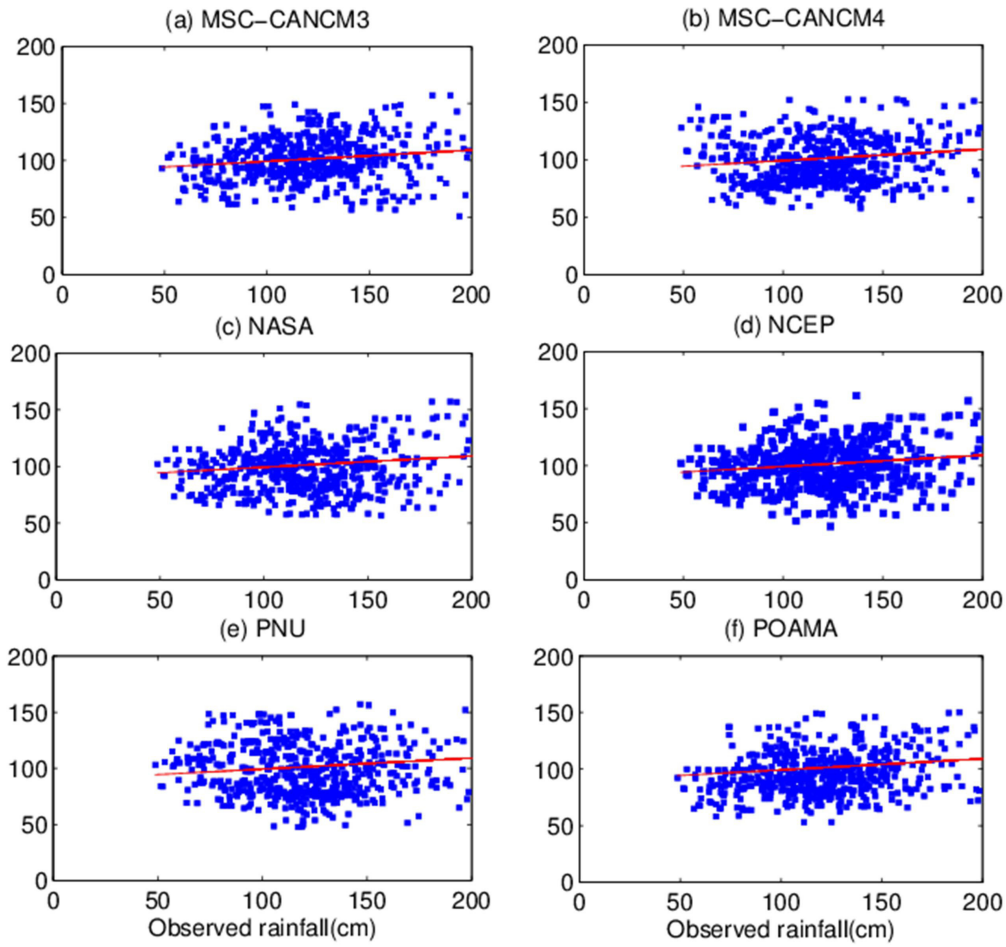

Figure 20. Scatter plot of seasonal total hindcast rainfall data against observed seasonal total rainfall data for 2000–2005, at a resolution of 0.25 × 0.25, in the main rice-growing region of South Korea.

3.3.2 Effect of the calibration method on the forecast skill

To evaluate how the calibration methods affect the forecast skill, the optimal YGP for each grid cell was firstly calibrated for two time periods, 1996–2000 and 2001–2005, for the same period as the yield data being used. Secondly, calibration of the YGP was based on cross validation of yield for two different time periods (1996–2000, 2001–2005), and the data for 1996–2000 was used to determine the 2001–2005 YGP, and vice versa. Figure 21 shows the correlation coefficient between observed and simulated yields obtained by driving the crop model with the ensemble mean of each single GCM and the multi-model. The forecast accuracy depends on the calibration method. Driving the model with the time dependent calibration of the YGP showed a higher skill than that with the calibration from the cross validation (Table 4). When the crop model was run with the cross calibrated YGP, the multi-model ensemble mean produced a higher correlation than the individual forecast model. This is probably because the multi-model ensemble mean can reduce the temperature error and spatial variability of temperature, and consequently produce a similar YGP for two different time periods. There was no significant correlation in the cross validation between the observed and simulated yield for some of the individual forecast models. This is possibly because there was a large difference in the YGP for the two periods when the cross validation was used. In contrast however, there was a significant correlation coefficient between the observed and simulated yields for all the forecast models when the optimal YGP for each grid cell was calibrated using the depend yield data. Therefore, the forecast skill of the crop model can be partly improved through calibration of the YGP based on the current yield, rather than on the yield from the previous period.

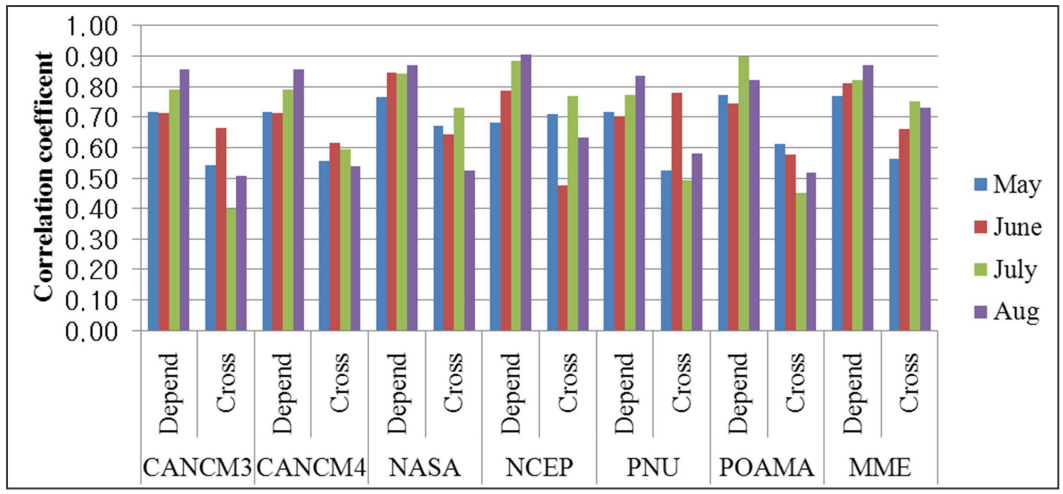

Figure 21. Correlation coefficient for the observed and simulated rice yields at the national level of South Korea from 1996 to 2005. Depend: the YGP of each grid cell was calibrated using the depend observed paddy rice yield for 1996–2000 and 2001–2005, Cross: calibration of the YGP is based on cross validation of the yield for 1996–2005.

Table 4. Correlation coefficient for observed and simulated rice yield and root mean square error between observed and simulated yield at the national level in South Korea, from 1996 to 2005. Depend: YGP of each grid cell was calibrated using depend observed paddy rice yield for 1996–2000 and 2001–2005; Cross: calibration of YGP is based on the cross validation of yield for 1996–2005. *p < 0.05, **p < 0.01

Model	Methods	Correlation coefficient				Root mean square error (RMSR) (kg/ha)			
		May	June	July	August	May	June	July	August
MSC-CANCM3	Depend	0.72*	0.71*	0.79**	0.86**	273	207	209	273
	Cross	0.54	0.67*	0.40	0.51	356	347	405	340
MSC-CANCM4	Depend	0.73*	0.76*	0.80**	0.87**	278	236	192	206
	Cross	0.56	0.61	0.59	0.54	346	367	328	337
NASA	Depend	0.77**	0.85**	0.84**	0.87**	212	150	250	224
	Cross	0.67*	0.64*	0.73*	0.52	260	285	290	314
NCEP	Depend	0.68*	0.79**	0.88**	0.90**	199	282	303	231
	Cross	0.71*	0.48	0.77**	0.63*	271	282	263	259
PNU	Depend	0.72*	0.70*	0.77**	0.84**	279	219	255	207
	Cross	0.52	0.78**	0.49	0.58	382	303	348	286
POAMA	Depend	0.77**	0.74*	0.90**	0.82**	193	269	220	245
	Cross	0.61	0.58	0.45	0.52	241	392	374	332
MME	Depend	0.77**	0.81**	0.82**	0.87**	276	239	205	202
	Cross	0.56	0.66*	0.75*	0.73*	328	270	276	273

To determine how the calibration methods of YGP affect the forecast skill, the GLAM-Rice was run with the calibrated YGP using the multi-model ensemble mean and ensemble mean of each single GCM, respectively. Comparisons of correlation coefficients and root mean square errors for observed and simulated rice yield at the national level of South Korea from 1996 to 2005 are showed in Table 5, using the time dependent calibration method. The correlation coefficient between the observed and simulated yield is quite close for calibration of YGP from each single GCM and for the multi-model ensemble mean in relation to the update of the seasonal weather forecast in the early of growth season. However, for the August update, calibration of the crop model using individual GCMs resulted in a higher correlation than the calibration from the multi-model ensemble mean (Table 5). In all cases, the root mean square error from the multi-model ensemble mean was higher than that from each single GCM. There was a large difference between the observed and simulated yields in some years when the GLAM-Rice was run with the YGP from the multi-model ensemble mean, and yield was systematically underestimated by the forecast model (Figure 22a, 22c). In contrast, the forecast accuracy was greatly improved when driving the model using the calibrated YGP from each GCM (Figure 22b, 22d), because calibrating the YGP using each GCM can partly correct the bias of each individual GCM. Generally, calibration of the crop model using individual GCMs showed a higher forecast skill than calibration from the multi-model ensemble mean. Therefore, in the remaining part of the study, yield was simulated based on the calibration of the model using individual GCM calibrations.

When the GLAM-Rice was run with the YGP from the multi-model ensemble mean, each separate run used the same YGP. The difference in forecasted yield was caused by the difference in climate variables from each single GCM. There were large uncertainties in yield prediction due to uncertainty in weather, soil, crop management, and the crop model itself. However, the weather input represented the largest uncertainty. The uncertainty in yield prediction due to climate model formation was relatively small, as shown in Figure 22a and 22c. This is probably because the seasonal variability of temperature from each GCM was similar. The forecast model was run using the estimated solar radiation from sunshine duration for all runs, and as previously stated, irrigated paddy rice is not sensitive to rainfall. Therefore, the difference in the forecasted yield was mainly due to the difference in predicted temperature.

Table 5. Correlation coefficient for observed and simulated rice yield and root mean square error between observed and simulated yield at the national level in South Korea from 1996 to 2005. MME: a single pair of YGP values was calibrated using the multi-model ensemble mean. Each single GCM model was used to calibrate a pair of YGP values. *p < 0.05, **p < 0.01

Model	YGP from	Correlation coefficient				Root mean square error (RMSR) (kg/ha)			
		May	June	July	Aug	May	June	July	Aug
MSC-CANCM3	MME	0.72*	0.79**	0.66*	0.68*	373	380	422	405
	CANCM3	0.72*	0.71*	0.79**	0.86**	273	207	209	273
MSC-CANCM4	MME	0.71*	0.87**	0.78**	0.71*	388	316	400	310
	CANCM4	0.73*	0.76*	0.80**	0.87**	278	236	192	206
NASA	MME	0.78**	0.77**	0.87**	0.77**	393	413	348	366
	NASA	0.77**	0.85**	0.84**	0.87**	212	150	250	224
NCEP	MME	0.86**	0.83**	0.90**	0.76*	291	335	276	339
	NASA	0.68*	0.79**	0.88**	0.90**	199	282	303	231
PNU	MME	0.73*	0.84**	0.71*	0.74*	380	405	446	326
	PNU	0.72*	0.70*	0.77*	0.84**	279	219	255	207
POAMA	MME	0.76*	0.84**	0.70*	0.76*	338	345	419	236
	POAMA	0.77**	0.74*	0.90**	0.82**	193	269	220	245

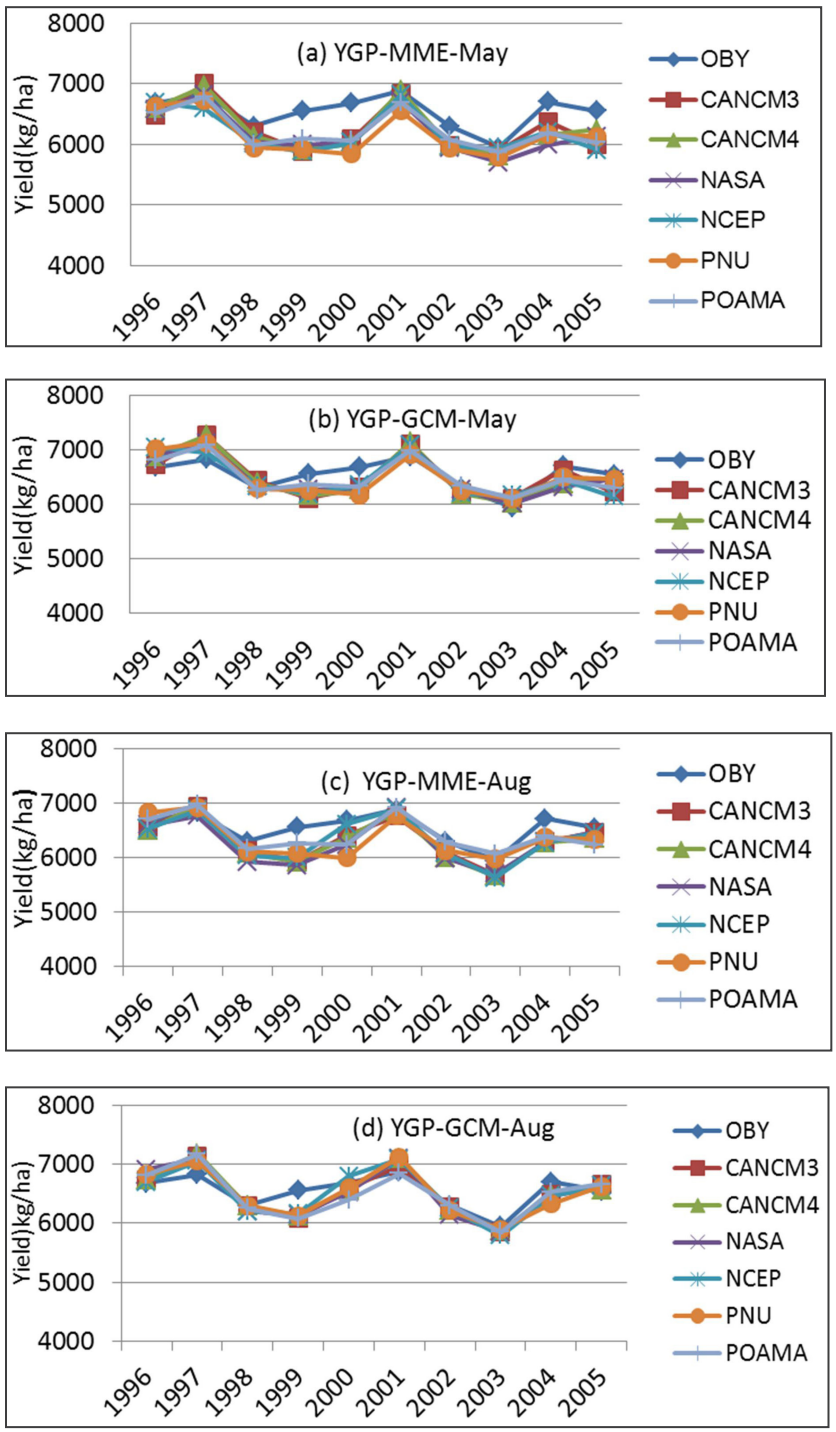

Figure 22. Comparison of observed (OBY) and simulated rice yield at the national level in South Korea from 1996 to 2005, when the GLAM-Rice was run with the seasonal forecast from six GCMs. (a) and (c) YGP values were calibrated using the multi-model ensemble mean; (b) and (d) each single GCM was used to calibrate a pair of YGP values.

3.3.3 Forecast skill of single GCM vs. MME

A comparison of forecast skill at the national level of South Korea for the multi model ensembles mean and single models (GCM) is shown in Table 6, where the GLAM-Rice model was run with a six-month forecast. It can be seen that NASA tends to produce a lower RMSE, and shows a higher correlation with the observations compared to the other single models at the national level in South Korea. When the forecast model was run using PNU, it showed a lower skill in terms of the correlation coefficient and RMSE. The multi model ensembles mean showed a similar skill to that of NASA, which was the single best model. This indicates that the multi model ensembles mean showed a good performance, and that it can be used to forecast the crop yield. A simulation performed by averaging the input of the crop mode from the multi model ensembles mean gave similar results to averaging the simulated output. Averaging the input or output was able to reduce the standard deviation of yield on a spatial scale, and improve the forecast skill slightly (Table 6). Overall, at the national level of South Korea, there was a minor difference in the forecast skill of the model when the GLAM-Rice was driven by each single GCM, and this is considered to be related to the bias correction of the individual models.

Table 6. Correlation coefficient between observed and simulated rice yield and root mean square error in yield at the national level of South Korea from 1996 to 2005. The GLAM-Rice was run with observed climate variables, and six months seasonal forecasts from six GCMs and the multi model ensembles mean. Abbreviations are: MME-IN: average input of the crop model from six GCMs; MME-OUT: average output of crop model from six GCMs, *p < 0.05, **p < 0.01

Data source	Correlation coefficient				Root mean square error(kg/ha)			
	May	June	July	Aug	May	June	July	Aug
Observation	0.82				180			
MSC_ CANCM3	0.72*	0.71*	0.79**	0.86**	273	207	209	273
MSC_ CANCM4	0.73*	0.76*	0.80**	0.87**	278	236	192	206
NASA	0.77**	0.85**	0.84**	0.87**	212	150	250	224
NCEP	0.68*	0.79**	0.88**	0.90**	199	282	303	231
PNU	0.72*	0.70*	0.77**	0.84**	279	219	255	207
POAMA	0.77**	0.74*	0.90**	0.82**	193	269	220	245
MME-IN	0.77**	0.81**	0.82**	0.87**	276	239	205	202
MMM-OUT	0.75**	0.80**	0.85**	0.87**	238	200	226	200

Figure 23 and Figure 24 show the correlation coefficient and model error between observed and simulated rice yield at a resolution of $0.25^{o} \times 0.25^{o}$, respectively, when the GLAM-Rice was run with a six months seasonal forecast from six GCMs and the multi model ensembles mean. Generally, the forecast skill was found to be relatively low, and the forecast error at individual grid cells was relatively large for the May update when driving the model with the observations and seasonal forecasts. When updating the seasonal forecasts with the observations however, the forecast skill improved, and consequently the forecast error was slightly reduced with the July update of the seasonal forecast, except for the MSC_CANCM3 July update (Figure 24). The correlation coefficient between the observed and simulated rice at a resolution of $0.25^{o} \times 0.25^{o}$ was quite similar between each single GCM and the multi model ensembles mean, except for the MSC_CANCM3 July update (Figure 23c). Therefore, driving the model using MSC_CANCM3 for the July update leads to a low forecast skill, and this is attributed to the lack of an adequate August temperature as predicted by MSC_CANCM3; the forecast skill actually improved with its August update. Simulation model errors can be due to either structural model errors from the crop model itself or from errors from the input datasets. Further updates of the seasonal forecast for August were not able to significantly reduce the forecast error, and this is considered to be possibly related to the crop model itself. The forecast skill of the GLAM-Rice was higher at the national level (Figure 22, Table 6) than at individual grid cells (Figure 23) in term of the correlation coefficient and root mean square error. When a forecast was conducted over a relatively larger spatial scale, the errors from difference sources were offset by each other.

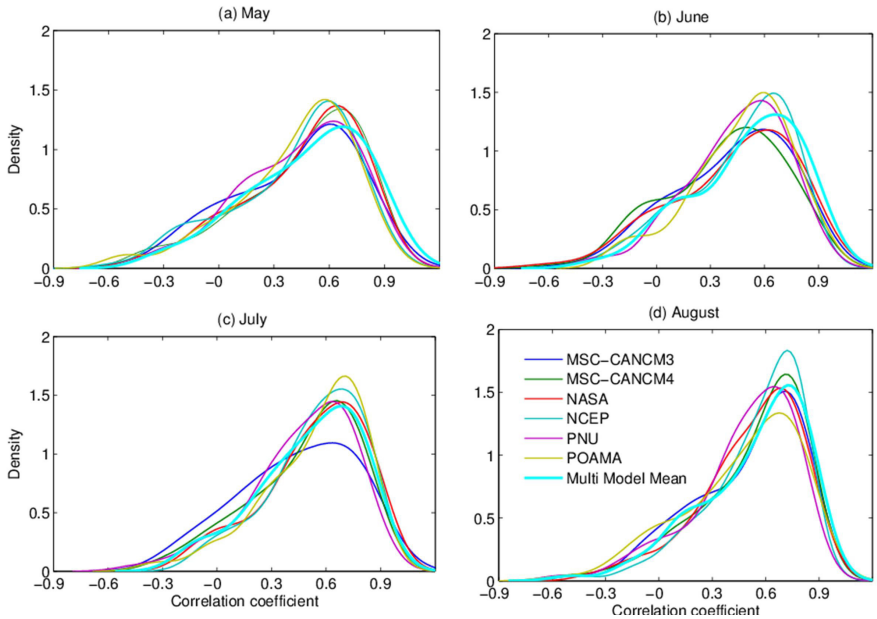

Figure 23. Density of correlation coefficient between observed and simulated rice yield at a resolution of 0.25° × 0.25° when the GLAM-Rice was run with six month seasonal forecasts from six GCMs and the multi model ensembles mean for 1996–2005. MME: average input of the crop model from six GCMs

The rice forecast for the May update was able to explain a significant portion of the variability of the observed yields at the national level of South Korea, both for single GCMs and for the multi model ensemble mean. The correlation coefficient between the observed and simulated yield was in the range of 0.68 to 0.77 ($p < 0.05$). Paddy rice is generally planted in May throughout the rice planting areas of South Korea. The forecast skill improved with successive monthly updates as the accuracy of seasonal forecast improved with updates using observations (Figure 25). The improvement in the forecast skill was mainly related to the update of temperature (because, as previously mentioned, rice is irrigated and it not sensitive to the amount of rainfall) and solar radiation from observations. Correlations showed the greatest increase with the July 1 update for most of the GCMs. July is the panicle differentiation period in most districts, and rice is quite sensitive to low temperature stress during this growth stage. Therefore, the accuracy of temperature in this period is extremely important in the determination of yield.

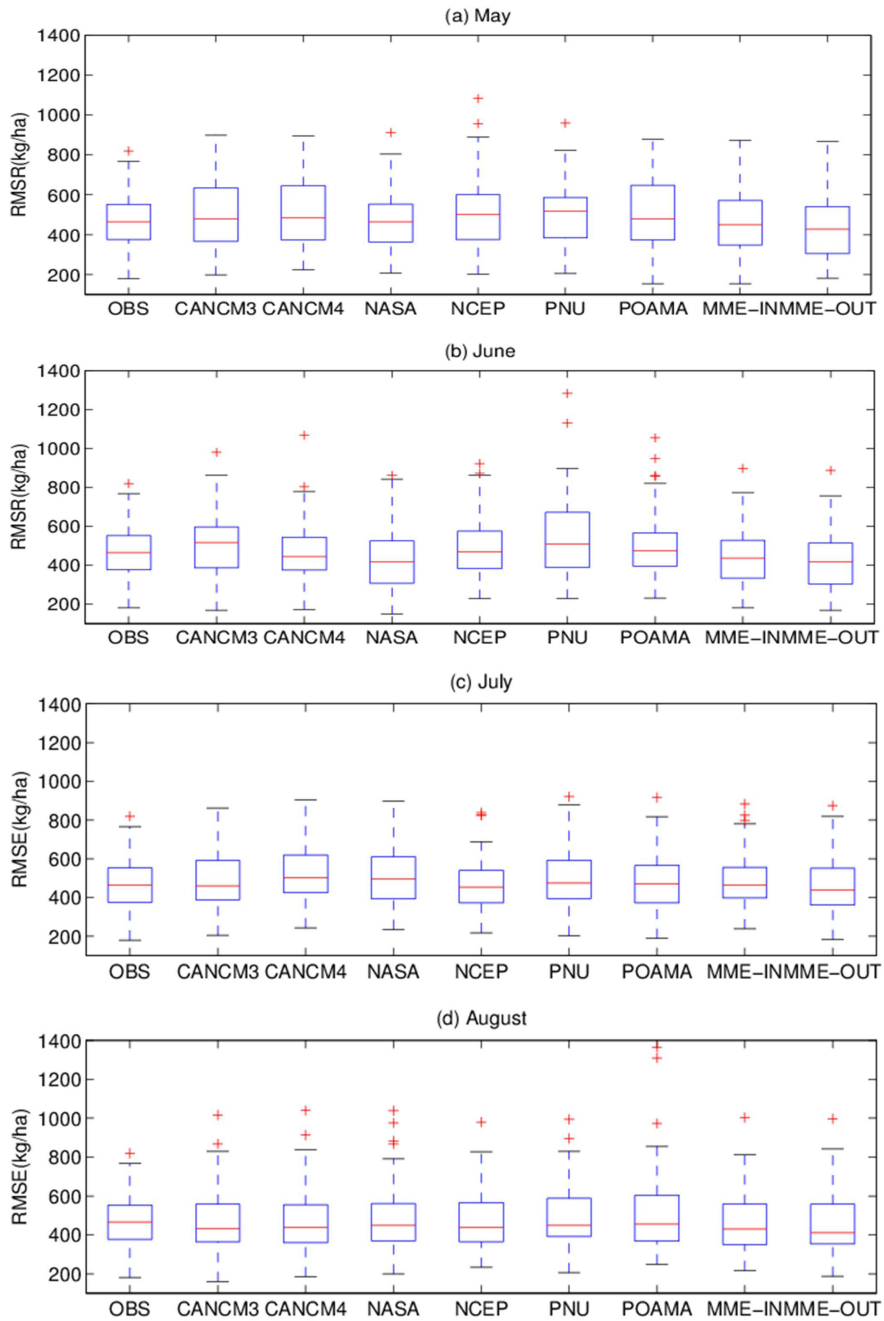

Figure 24. Box plot of RMSE between observed and simulated yield at a resolution of 0.25°× 0.25° from six GCMs and the multi model ensembles mean for 1996–2005.

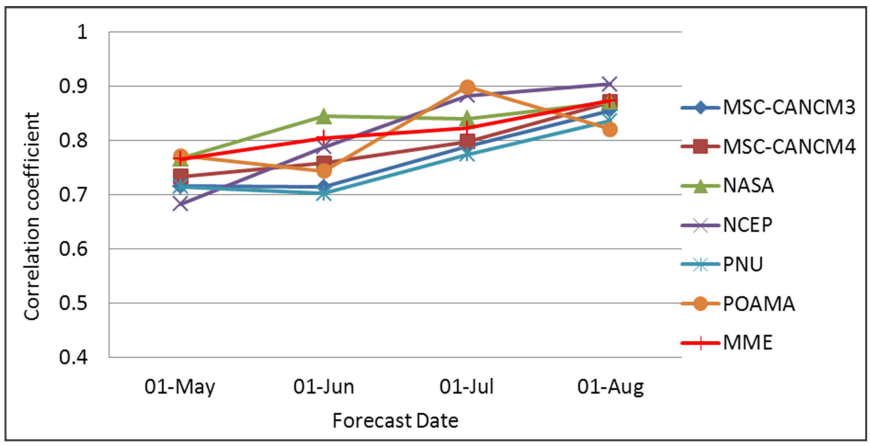

Figure 25. Correlation coefficient between observed and simulated rice yield at the national level of South Korea from 1996 to 2005 with successive monthly updates of seasonal forecast using observations from May 1 to August 1.

Correlations of predictions of observed yields using the May update (Figure 26) showed less homogeneity in space for each GCM. This is likely to be due to the heterogeneity of homogeneous regional conditions, such as climate, soil, and field management processes. Correlations between the predicted and observed yield increased with subsequent updates (Figure 27), but the increase in forecast accuracy from May to June was less significant than that from June to August. This is likely to be because the accuracy in later seasonal temperature is more important for simulating crop yield. Correlations between predictions and observations increased with the update of forecast from May 1 to August 1, and the August update showed more spatial homogeneity (Figure 27).

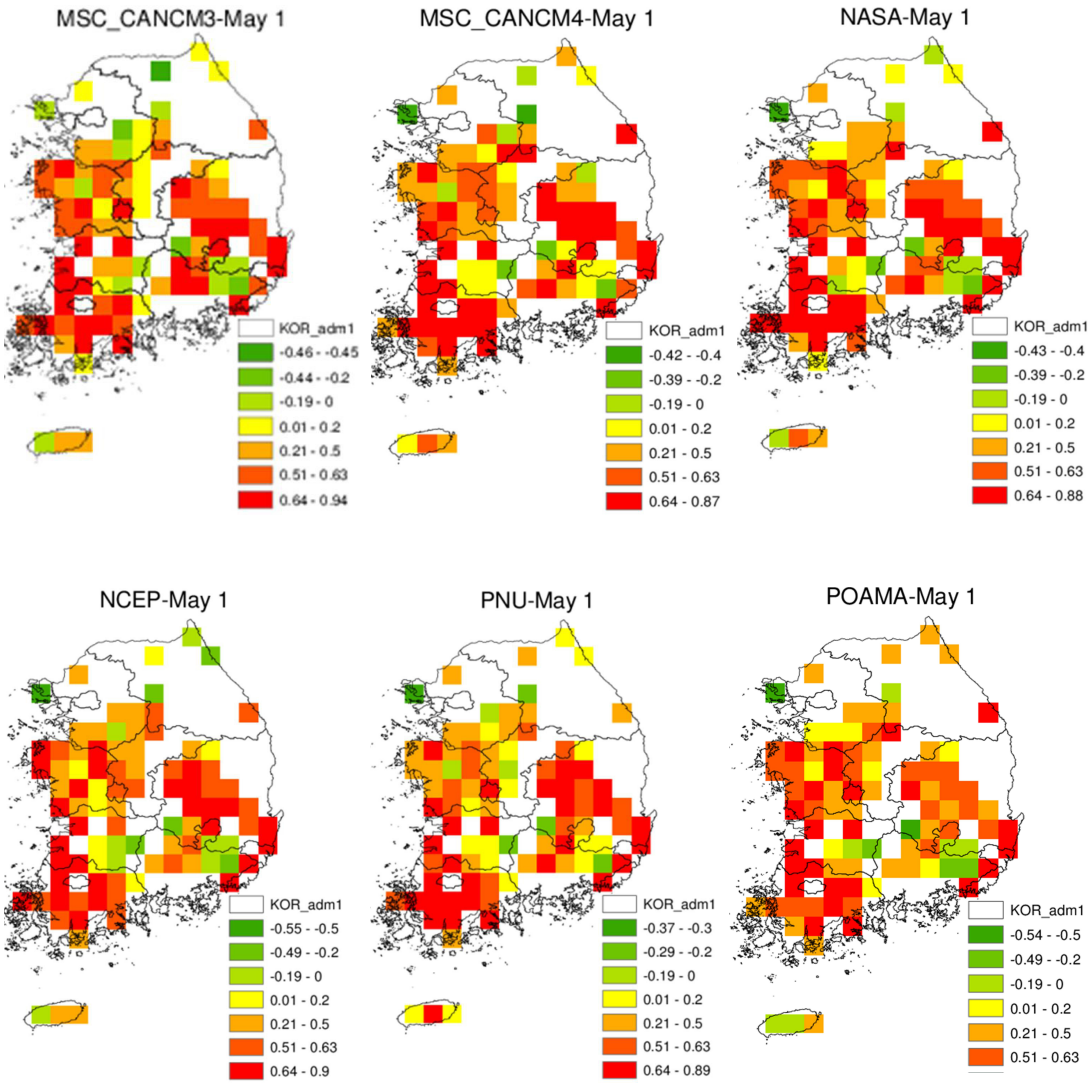

Figure 26. Correlation of predictions with observed yields at a resolution of 0.25°× 0.25° with the May 1 update of the forecast, using observations for 1996–2005. The GLAM-Rice was run with the seasonal forecast from six GCMs, respectively.

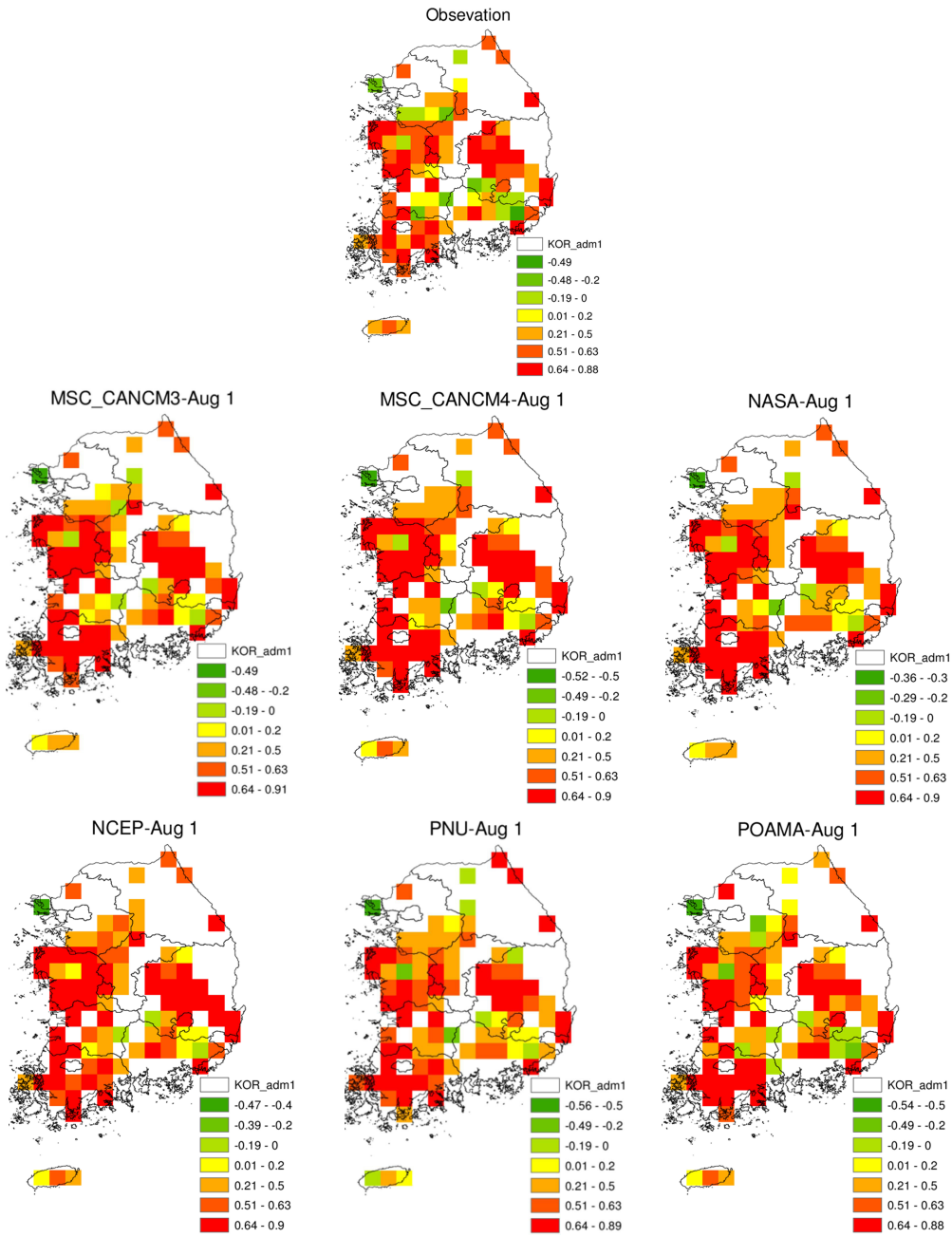

Figure 27. Correlation of predictions with observed yields at a resolution of 0.25° × 0.25° for 1996–2005 using the August update of forecast with observations. The GLAM-Rice was run with observations and seasonal forecasts from six GCMs, respectively.

Two simulations were conducted for each set of hindcast for the three months seasonal forecast, in order to predict rice from August. In the first experiment, the three months seasonal forecast was used before August, and after August, it was used in cases where observed weather data was not available before August. There was a significant correlation coefficient (0.65–0.82) between the observed and simulated rice yield (Table 7) in 9 out of 10 GCMs at the national level of South Korea from 1996–2000 (Figure 28). Driving the crop with POAMA produced a higher RMSE, and showed a lower correlation with observations compared to the skills of the other models. There was a higher correlation ($r = 0.78–0.82$, $p < 0.001$) between the predicted and observed rice yields when the GLAM-Rice was run with CWB, NCEP, and SCM. This indicates that without using the update of seasonal forecasts with the observations, the three months seasonal forecast can be used to forecast rice yield in August for some of the GCMs, but not all of them.

In the second experiment, the seasonal forecast was updated with the observation before 31 July, and after this date, the seasonal forecast was used until harvest. The forecast skill of the crop model largely improved with August updates, as the accuracy of the seasonal forecast improved with the update using observations (Figure 28).

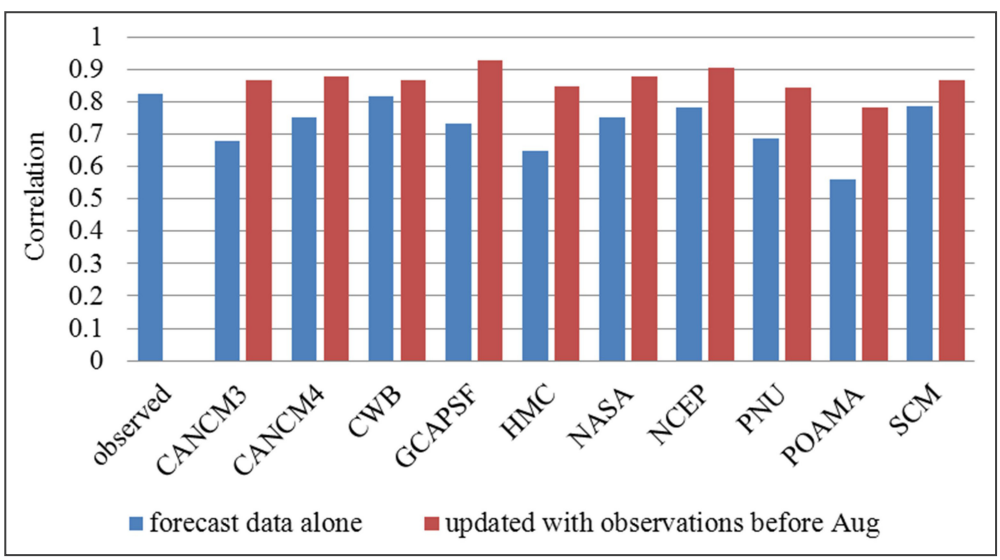

Figure 28. Correlation coefficient between observed and predicted rice yield and root mean square error in yield at the national level in South Korea from 1996 to 2005. The GLAM-Rice was run with observed climate variables, and the three months seasonal forecast from ten GCMs

Table 7. Correlation coefficients between observed and predicted rice yield and root mean square error in yield at the national level of South Korea from 1996 to 2005. The GLAM-Rice was run with observed climate variables, and the three months seasonal forecast from ten GCMs, *p < 0.05, **p < 0.01

Data source	Three months seasonal forecast		Three months seasonal forecast with August update	
	Correlation	RMSE	Correlation	RMSE
Observations			0.82**	180
MSC_CANCM3	0.68*	247	0.87**	197
MSC_CANCM4	0.75*	258	0.88**	205
CWB	0.82**	203	0.87**	211
GCAPSF	0.73*	276	0.93**	369
HMC	0.65*	256	0.85**	213
NASA	0.75*	261	0.88**	219
NCEP	0.78**	228	0.90**	193
PNU	0.69*	267	0.84**	218
POAMA	0.56	289	0.78**	223
SCM	0.78**	227	0.87**	228

3.3.4 The effect of solar radiation on forecast skill

To examine how the accuracy of solar radiation affects the forecast skill of the crop model, the GLAM-Rice was run with the original solar radiation and the climatology of solar radiation, respectively. The original solar radiation refers to estimated solar radiation from measured sunshine duration using the Angstron-type regression. The climatology of solar radiation is the multi-yearly averaged daily solar radiation over the period 1996 to 2005. When the GLAM-Rice was run with the original solar radiation, there were significant correlations between the observed and the predicted rice yield at the national level of South Korea (Table 8); the predicted yield was able to capture most of the variability of the observed yield (Figure 29a). However there were no significant correlations between the observed and predicted yields at the national level of South Korea when driving the crop model with the climatology of solar radiation (Table 8), and the variability of the yield was underestimated by the model (Figure 29b). When forcing the GLAM-Rice with the climatology of solar

radiation, the model showed low skill, both at the national level of South Korea and within individual grid cells. When the GLAM-Rice was forced by the climatology of solar radiation, only 0–11 % of the grid cells showed significant correlations between the observed and predicted rice yields at a resolution of 0.25° × 0.25° for South Korea from 1996 to 2005. The temperature was a dominant climate variable, affecting the variability of the rice yield in a small number of grid cells. In contrast, the proportion of grid cells that showed significance for the observed and predicted yield correlation greatly increased from 24% for POAMA to 36% for MME by driving the model with original solar radiation (Figure 30). This indicates that the forecast skill of the GLAM-Rice has a higher association with solar radiation than with temperature; therefore, providing reliable solar radiation is critical for improving the forecast skill of the GLAM-Rice.

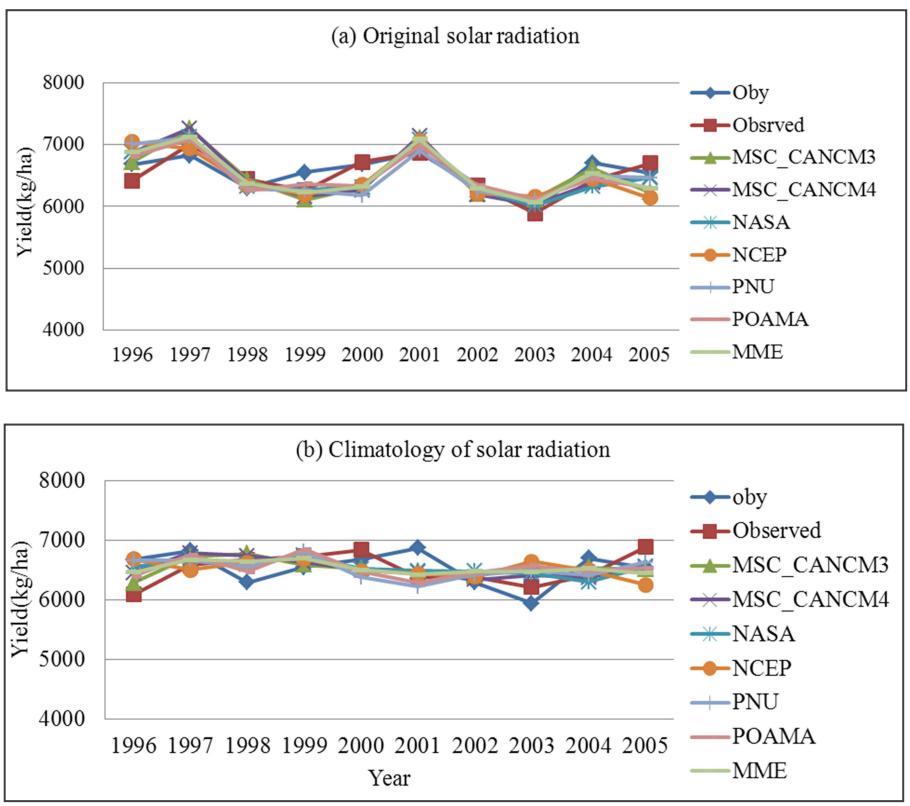

Figure 29. Comparison of observed and predicted national rice yield in South Korea for 1996–2005 by forcing the GLAM-Rice with the original solar radiation and climatology of solar radiation, respectively. The seasonal forecast from each GCM and MME were updated with observations on May 1. Abbreviations are as follows, Oby: observed rice yield; Observed: the crop model was forced by observed climate variables

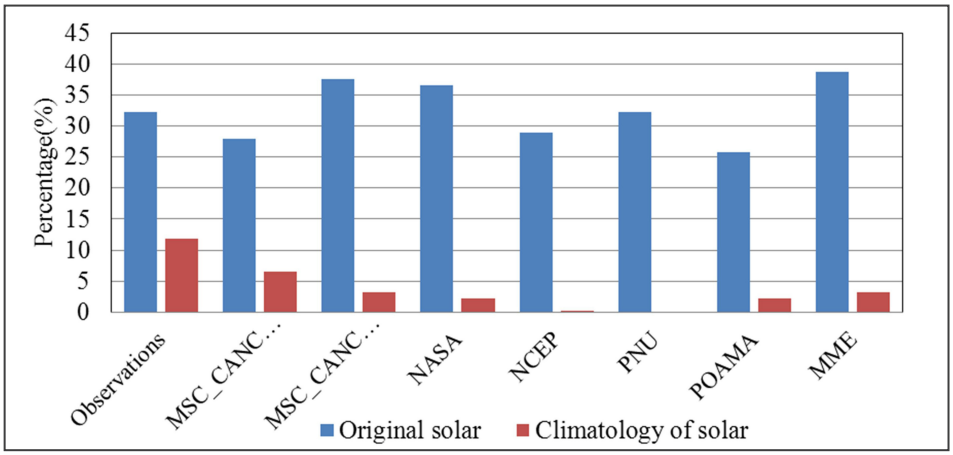

Figure 30. A comparison of the percentage (%) of grid cells that were significant at the 5% significance level for relationships between observed and predicted rice yields with a May update at a resolution of 0.25° × 0.25° for South Korea from 1996 to 2005. The GLAM-Rice was run with original solar radiation and the climatology of solar radiation, respectively.

Table 8. Correlation coefficient between the observed and simulated rice yields and the root mean square error in yield at the national level of South Korea from 1996 to 2005. The GLAM-Rice was run with original solar radiation and the climatology of solar radiation, respectively.

Data source	Correlation coefficient		Root mean square error (RMSR) (kg/ha)	
	Original solar	Climatology of solar	Original solar	Climatology of solar
Observations	0.82**	0.18	180	336
SCM_CANCM3	0.72*	-0.01	273	304
SCM_CANCM4	0.73*	0.21	278	278
NASA	0.77**	0.14	212	281
NCEP	0.68*	-0.24	199	331
PNU	0.72*	-0.09	279	329
POAMA	0.77**	-0.10	193	326
MME	0.77**	0.05	276	282

3.4 MODIS derived LAI

The satellite derived LAI is used to force the GLAM-Rice to test if there are any improvements in the rice yield forecasts. Firstly, the correlation between rice yield and the maximum LAI at the resolution of 0.25° × 0.25° was examined in the main rice-growing region of South Korea from 2000 to 2009. Results showed a weak correlation between rice yield and maximum LAI for most of grid cells (Figure 31). This is considered likely due to either the quality of MODIS LAI at the 1 km × 1 km resolution, or the reason that the resolution of 0.25° × 0.25° is not appropriate. As shown in Figure 32, the observed LAI was lower in comparison with that of the MODIS LAI. To assess the forecast skill of the GLAM-Rice with MODIS LAI, two experiments were carried out. In the first experiment, the GLAM-Rice was run with the simulated LAI from the model itself. In the second experiment, the simulated LAI from the GLAM-Rice was replaced by the MODIS-derived LAI. The results showed that forcing the GLAM-Rice using the satellite derived LAI made no improvement to the forecast skill of the model (Figure 33), and this is probably related to the data quality of MODIS-derived LAI in relation to the inhomogeneous land cover, or to the insufficient spatial resolution of the input.

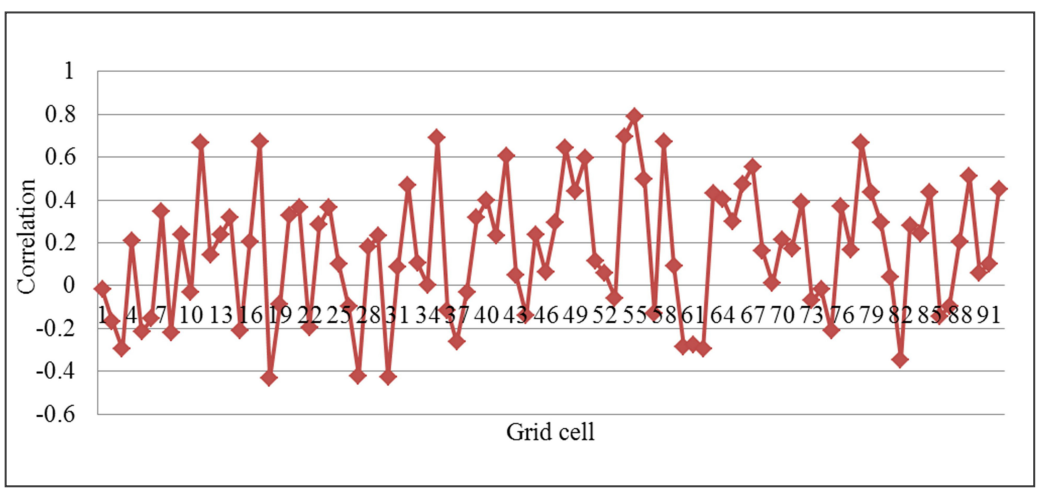

Figure 31. Correlation coefficient between rice yield and maximum LAI at a resolution of 0.25° × 0.25° in the main rice-growing region of South Korea, from 2000 to 2009.

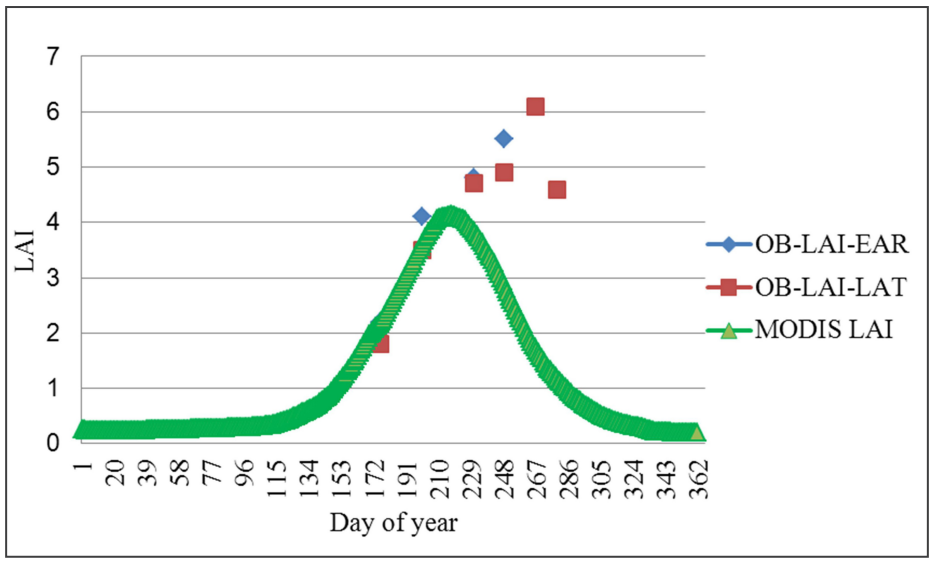

Figure 32. Comparison of MODIS LAI and observed LAI (2005) in Dangjin County, South Korea. Abbreviations are as follows, OB-LAI-EAR: observed LAI for earlier maturity variety; OB-LAI-LAT: observed LAI for later maturity variety. The observed LAIs are from Jang et al (2012).

Figure 33. Comparison of observed and predicted rice yield for 2000–2009 by driving the GLAM-Rice with the satellite-derived LAI, and LAI from the crop model, respectively. Abbreviations are as follows, Oby: observed rice yield; GLAM-LAI: LAI is simulated by the crop model; MODIS-LAI: LAI from the crop model was replaced with the satellite-derived LAI

4. CONCLUDING REMARKS

Our results show that there is a significant correlation between rice yield and intercepted solar radiation for 1996–2010 at the national level of South Korea. From 1996 to 2010 the intercepted solar radiation, temperature, and the interaction between intercepted solar radiation and temperature explained approximately 42%, 16%, and 17% of the variability in rice yield, respectively. This indicates that solar radiation is one of the most important climate variables affecting the variability of the paddy rice yield for the period 1996–2010 in South Korea. Accurate values of solar radiation are therefore required to make a reliable crop forecast. However, solar radiation is currently only available at a limited number of stations in South Korea, whereas sunshine records are available from all stations, and therefore the measured sunshine duration was used to estimate global solar radiation using the modified form of Angstron-type regression. In general, the modified form of the Angstron-type regression equation led to reasonable estimations of daily solar radiation. The coefficient of determination R^2 between the estimated and measured daily solar radiation at 18 meteorological stations varied from 0.68 for Suwon, to 0.816 for Jeju from 1985 to 2010. It may therefore be concluded that the Angstron-type regression equation presented in this study can be used reasonably well for estimating solar radiation at a given location, and possibly in other regions with similar climatic conditions.

When the GLAM-Rice was driven by the estimated solar radiation, the correlation coefficients between observed and simulated rice at a resolution of $0.25^{o}\times0.25^{o}$ were obviously higher that from the ERA-Interim solar radiation. Running the GLAM-Rice with the estimated solar radiation greatly improved its skill, both at the individual grid cell and at the national level. This indicates that making improvements in the accuracy of solar radiation is quite important for the skill of the paddy rice yield forecast. However, both the sunshine duration and solar radiation are not provided by the GCMs for the operational seasonal forecast of climate, and they generally only provide the seasonal forecast of temperature and rainfall. Therefore, it is necessary to further examine how to estimate solar radiation using limited climate variables such as temperature and rainfall.

In order to estimate how the accuracy of temperature affects the performance of the GLAM-Rice in rice yield forecasting, the GLAM-Rice was run using the nearest neighbor

interpolated temperature and the PRIDE downscaled temperature, respectively. When using the nearest neighbor interpolated temperature, the forecast skill of the model was improved compared to when the downscaled temperature of PRIDE was used, both at the individual grid cell and at the national level of South Korea. This is considered to be probably related to the fact that the nearest neighbor interpolated temperature can represent the mean temperature in the main rice planting region, while the PRIDE downscaled temperature delivers the spatial averages. In general, the PRIDE downscaled temperature was lower than that from the nearest neighbor interpolation, especially for the low temperature region. The implication of this is that the gridded climate variables, such as temperature, at a relatively larger scale cannot be used to simulate the crop yield in the regions where the topography is complex.

To illustrate how the spatial scale of climate variables affects the forecast skill of a dynamical regional crop model, the GLAM-Rice was run with the gridded climate data at a smaller resolution of 0.25°×0.25° and then coarser resolutions of 0.5°×0.5° and 1°×1°. A comparison of the integrated national yield showed that driving the GLAM with the 0.25° ×0.25° resolution climate data resulted in slightly higher correlations between the observed and simulated rice yields. However, when the resolution of climate date was increased from 1°×1° to 0.5°×0.5° and 0.25°×0.25°, there was limited improvement in the forecast skill of the model. This is because paddy rice is grown under irrigated conditions, and is therefore not sensitive to rainfall, but is sensitive to temperature and solar radiation. Temperature and solar radiation are smooth variables on a spatial scale, and variability in the spatial scale is relatively small, the forecast skill of the GLAM-Rice shows limited sensitivity to change related to the spatial scale of climate variables between the smaller 0.25°×0.25° resolution and the coarser 1°×1° resolution. This indicates that the coarser 1°×1° resolution's climate variables can be used to forecast rice yield for South Korea and for similar crop environmental regions.

In order to demonstrate if the monthly averaged climate variables could be used to forecast the crop yield, the dynamical crop model was run with the daily and 30-day averagedrainfall, respectively, and results showed a similar yield when the model was run using the 30-day averaged rainfall and original daily rainfall. However, driving the model with the 30-day averaged temperature or solar radiation led to a larger difference compared to the predicted yield using daily temperature or daily solar radiation. This indicates that the

monthly average rainfall can be used to forecast the irrigated paddy rice yield. However, the monthly averaged temperature and solar radiation cannot be used to forecast the rice yield, because averaging the daily temperature or solar radiation over time may progressively filter out short-term variability and ignore the low temperature/solar radiation stress, consequently overestimating the crop yield. Therefore, the monthly averaged rainfall can be used in the crop model for a rice yield forecast, although the provision of accurate daily temperature and solar radiation are also required to provide an accurate rice yield forecast.

To evaluate how the calibration method affects the forecast skill, the time dependent and independent calibrations of YGP were carried out, respectively. The forecast accuracy of the GLAM-Rice is dependent on the calibration method. The GLAM-Rice based on calibration with the YGP from the same period as the yield data used showed a significantly higher skill than that for the independent calibration, which showed no significant correlation between the observed and simulated yields while driving the crop model with most of the climate forecast models. It is possible that there was a large difference in the YGP for two periods 1996–2000 and 2001–2005 when the independent validation was used, and therefore the forecast skill of the crop model could be partly improved through calibration of the YGP based on current yield rather than using the yield from a previous period.

To determine how the calibration method of the YGP affects the forecast skill, the GLAM-Rice was run with the calibrated YGP using the multi-model ensemble mean and each single GCM model, respectively. Calibration of the crop model using individual GCMs resulted in higher correlation than calibration from the multi-model ensemble mean. The forecast accuracy greatly improved when driving the model using the calibrated YGP from each GCM, because the calibration of YGP using each GCM can partly correct the bias of each individual GCM. Therefore, the seasonal crop forecast needs to be based on calibration of the model using individual GCM calibrations, rather than using the multi-model ensemble mean.

For the six month forecast overall at the national level of South Korea, each GCM performed very similarly in terms of the crop yield forecasting skills. NASA showed a higher correlation with observations compared to other single models, while PNU showed a lower forecasting skill. The multi model ensembles mean showed a similar skill to that of the

single best model NASA. The simulation when driving the crop model with the multi model ensembles mean resulted in similar results as averaging the simulated output of each single GCM. The forecast skill improved when updating the seasonal forecast with the observation, and consequently the forecast error can be slightly reduced with the June update of the seasonal forecast. Further updates of seasonal forecasts cannot significant reduce the forecast error, and this is perhaps because the forecast error is from the crop model itself. The forecast skill of the GLAM-Rice is higher at the national level than at the individual grid cell level, because when a forecast is conducted over a relatively larger spatial scale, the errors from difference sources can be offset by each other. As shown by the previous study of Li et al. (2007) the GLAM has a higher skill at the regional level than at the field scale because the skill of the GLAM model depends on the correlation between crop and climate. Generally, there is higher correlation between crop and temperature at the larger spatial than at the smaller scale (Li et al. 2010b). Similarly Hansen et al. (2004) showed that the prediction accuracy was generally higher at the state scale than at the smaller district scale.

At the national level of South Korea, the rice forecast for the May update can explain a significant portion of variability of the observed yields, both for single GCMs and for the multi model ensembles mean. This indicates that the rice yield can be predicted early in the growing season. The forecast skill improved with successive monthly updates, as the accuracy of the seasonal forecast improved with updates of the seasonal forecast using observations. Correlations showed that the greatest increase in the forecasting skill occurred with the July 1 update for most of the GCMs, because the temperature in July is quite important for rice growth. Correlations of predictions with observed yields at the level of the individual grid cells, showed less homogeneity in space for each GCM with the May update. This is likely to be due to the heterogeneity of the homogeneous regional conditions, such as climate, soil, and field management. Correlations between the predicted and observed yields increased with subsequent updates, and the August update showed better homogeneity in space. While forcing the GLAM-Rice with the climatology of solar radiation, the model showed low skill, both at the national level and in individual grid cells for South Korea. This indicates that the forecast skill of the GLAM-Rice has a higher association with solar radiation than with temperature for 1996–2005. Providing reliable solar radiation is therefore proven to be critical for improving the forecast skill of the GLAM-Rice. We can conclude that if reliable

solar radiation can be provided, there is a practical feasibility of using properly downscaled multi-model ensemble seasonal forecasts from GCMs for predicting crop yields early in the crop-growing season, which is important. Once a reasonable seasonal climate forecast is provided, the GLAM-Rice model will be capable of adequately capturing the variability of the observed paddy rice yield early in the growing season at a large spatial scale. Consequently, the regional rice model GLAM-rice could then be transferred and delivered to APCC product users/stakeholders for regional rice forecasting, which would provide potentially valuable information for farms and other agricultural stakeholders for the management of risk and improvements in decision making.

The three-month seasonal forecast can be used to forecast rice in the middle of the rice growing season from August. Without updates of the seasonal forecast with observations before August, there was a significant correlation coefficient between the observed and simulated rice yields in 9 out of 10 GCMs at the national level of South Korea. This indicates that without updates of seasonal forecasts with observations, the three months seasonal forecast can be used to forecast the rice yield in August for some of the GCMs, but not for all of them. The forecast skill of the crop model largely improved with August updates, as the accuracy of the seasonal forecast improved when using the updates with observations.

There is a weak correlation between the rice yield and the maximum LAI for the most of grid cells. At the representative site of South Korea, the observed LAI was greater than that of MODIS LAI. The satellite-derived LAI was used to force the GLAM-Rice to test if the rice yield forecasts could be improved, and results showed that no improvement was made in the forecast skill of the model. This is considered to be probably caused by either the data quality of MODIS derived LAI, inhomogeneous land cover, or the insufficient spatial resolution of inputs.

The forecast skill of the GLAM-Rice is affected by the accuracy of the input dataset, the spatial and temporal scales applied, and the formation of the crop model itself. The accuracy of input information, for example weather data, cannot necessarily represent the temperature or solar radiation in main cropping areas, also uncertainties in the sowing and harvest date can greatly affect the model's performance. Therefore, further improvement in the existing yield forecast methods requires reliable input data for calibration, such as crop yield statistics

and improved maps of soil types. In addition, the impact of damage from pests and diseases, which is related to weather conditions, is not included in the model. However, it is of note that the issue of extreme events, such as wind and frost, which have been important factors affecting the rice yield in the South Korea in some years, has not been addressed in this study because of the limited time series of crop yield and seasonal forecasts from the GCMs. The parameterization of low and high temperature stress needs further calibration and validation under various environmental conditions, based on field experimental datasets.

Acknowledgement

We wish to thank Dr. Jaepil Cho from the APCC for providing the downscaled daily seasonal forecast datasets for 57 stations in South Korea.

Appendix A

Original values for the parameters used in GLAM by Challinor et al. (2004) for groundnut. Values in square brackets are the calibrated values.

Parameters	Description	Value
L_{cr}	Critical threshold value of L	0.7
T_{Tmax}	Maximum possible potential transpiration rate	0.15–0.4(cm day^{-1})
α	Priestley–Taylor coefficient	1.26
A	Mean albedo of the surface	0.2
C_G	Constant for the soil heat flux	0.4
k	Extinction coefficient	0.2–0.8 [0.5]
P_{cr}	Threshold of daily total rainfall	0.1(cm)
k_{DIF}	Uptake diffusion coefficient	0.06 cm^2 day^{-1}
C_θ	Constant for critical extractable soil water	0.5
z_{max}	Depth of soil profile	210 (cm)
N_{SL}	Number of soil layers	25
C_{d1}	Constant for drainage	2.96 (day^{-1})
C_{d2}	Constant for drainage	−2.62 (day^{-1})
C_{d3}	Constant for drainage	0.85 (day^{-1})
K_{ks}	Constants for soil hydraulic conductivity	37(cm day^{-1})
z_{ed}	Depth of soil from which evaporation occurs	16.8 (cm)
C_V	Constant for vapor pressure deficit	0.7

Appendix B

New parameter value for rice in GLAM

Parameters	Description	Value	Source
DLDTMX	Maximum LAI expansion rate	0.08-0.18	Calibration
TE	Transpiration efficiency (kPa kg m^{-3})	6	Sinclair, 1998
P_TRANS_MAX	Max value of pot. Trans (cm)	0.6	Wang et al. 2004
TEN –MAX	Maximum Transpiration efficiency (g kg^{-1})	5.9	Yoshida 1975
DHDT	Rate of change in harvest index	0.01	calibration
C_{ph}	Critical photoperiod (hours)	11.5	Bouman et al. 2001
TB	Base temperature(°C)	8	Gao et al. 1992
TO	Optimum temperature (°C)	30	Gao et al. 1992
TM	Maximum temperature (°C)	42	Gao et al. 1992
T_{max}	Maximum temperature for flowing (°C)	35	Matsui and Horie 1992
ZRTTR	root depth at transplanting (m)	0.05	Boling et al. 2000
ZSMAX	Maximum root length (cm)	57	Chaitra et al. 2006

REFERENCES

Abawi, G. Y., R. J. Smith, and D. K. Brady, 1995: Assessment of the value of long range weather forecasts in wheat harvest management. *J. Agric. Eng. Res.* **62**, 39–48.

Arya, S. P., 1988: *Introduction to Micrometeorology*. Academic Press, San Diego, CA, 307 pp.

Batjes, N. H., 1997: A world dataset of derived soil properties by FAO-UNESCO soil unit for global modelling. *Soil Use Manage* **13**, 9−16

Becker-Reshef I., E. Vermote, M., Lindeman, and C Justice, 2010: A generalized regression-based model for forecasting winter wheat yields in Kansas and Ukraine using MODIS data. *Remote Sens Environ*, **114**, 1312−1323

Boling, A., T. P. Tuong, B. A. M. Bouman, M. V. R. Murty, and S. Y. Jatmiko, 2000: Effect of climate, agrohydrology and management on rainfed rice production in Central Java, Indonesia: a modeling approach. *Proc. of the International Workshop on Characterizing and Understanding Rainfed Environments*, Bali, Indonesia. Los Baños (Philippines), International Rice Research Institute, 5.

Bolton, D., 1980: The computation of equivalent potential temperature. *Monthly Weather Rev.*, **108**, 1046–1053.

Bouman B., C. Diepen, P. Vosen, and T. van Der Wal, 1995: Simulation and system analysis tolls for crop yield forecasting. In: *Application of systems approaches at the farm and regional levels, Vol.* 1. Kluwer, Dordrecht, 325–340.

Bouman, B. A. M., M. J. Kropff, T. P. Tuong, M. C. S. Woperis, H. F. M. ten Berge, and H. H. van Laar, 2001: *Modelling Lowland Rice*. International Rice Research Institute, Los Banos, Philippines; and Wageningen University and Research Centre, Wageningen, The Netherlands, 235 pp.

Brisson, N., C. Gary, E. Justes, R. Roche, B. Mary, D. Ripoche, D. Zimmer, J. Sierra, P. Bertuzzi, P. Burger, F. Bussière, Y.M. Cabidoche, P. Cellier, P. Debaeke, J. P. Gaudillère, C. Hénault, F. Maraux, B. Seguin and H. Sinoquet, 2003: An overview of the crop model STICS. *Eur. J. Agron.*, **18**, 309–332.

Chaitra, J., M. S. Vinod, N. Sharma, S. Hittalmani, and H. E. Shashidhar, 2006: Validation of markers linked to maximum root length in rice (*Oryza sativa L.*). *Curr. Sci.*, **90**, 835–838.

Challinor A. J., Wheeler T.R., Craufurd P. Q., Slingo J. M., and Grimes D. I. F., 2004: Design and optimisation of a large-area process-based model for annual crops. *Agric Forest Meteorol*, **124**, 99–120.

Challinor, A. J., J. M. Slingo, T. R. Wheeler, and F. J. Doblas-Reyes, 2005: Probabilistic simulations of crop yield over western India using the DEMETER seasonal hindcast ensembles. *TELLUS A*, **57**, 498–512.

Chipnashi, A. C., E. A. Ripley, and R. G. Lawford, and R. G., 1999: Large-scale simulation of wheat yields in a semi-arid environment using crop-growth model. *Agric. Syst*, **59**, 57–66.

Choudhury, B. J., S. B. Idso, and R. J. Reginato, 1987: Analysis of an empirical model for soil heat flux under a growing wheat crop for estimating evaporation by an infrared temperature based energy balance equation. *Agric. Forest Meteorol*, **39**, 283–297.

Doraiswamy, P. C., S. Moulin, P.W. Cook, and A. Stern, 2003: Crop yield assessment from remote sensing. *Photogramm Eng Rem S*, **69**, 665–674.

Duffie J. A., and W. A. Beckman, 1994: *Solar Engineering of thermal Processes, 2nd Edn*. John Wiley, New York

Ferris, R., R. H. Ellis, T. R. Wheeler, and P. Hadley, 1998: Effect of high temperature stress at anthesis on grain yield and biomass of field-grown crops of wheat. *Ann. Bot.*, **82**, 631–639.

Gao, L. Z., Z. Q. Jin, Y. Huang, and L. Z. Zhang, 1992: Rice clock model: a computer model to simulate rice development. Agric. *Forest Meteorol*, **60**, 1–16.

Hammer, G.L., and R.C. Muchow, 1991: Quantifying climatic risk to sorghum in Australia's semiarid tropics and subtropics: model development and simulation. *Climatic Risk in Crop Production: Models and Management for the Semiarid Tropics and Subtropics*, R.C. Muchow, and J.A. Bellamy, Eds., CAB International, 205–232

Hansen, J. W., A. Potgieter, and M. K. Tippett, 2004: Using a general circulation model to forecast regional wheat yields in northeast Australia. Agric. *Forest Meteorol.* **127**, 77–92.

Horie, T, M. Yajima, and H. Nakagawa, 1992: Yield forecasting. *Agric. Sys.*, **40**, 211–236.

IPCC, 2013: *Climate Change 2013: The Physical Science Basis*. Report Intergovernmental Panel on Climate Change (IPCC).

Islam, M. S. and J. I. L. Morison, 1992: Influence of solar radiation and temperature on irrigated rice grain yield in Bangladesh. *Field Crops Research*, **30**, 13–28,

Jang, M. W., Y. H. Kim, N. W. Park, and S. Y. Hong, 2012: Mapping Paddy Rice Varieties Using Multi-temporal. *Korean J. Remote Sens*, **28**.653-660

Jones, J. W., G. Hoogenboom, C. H. Porter, K. J. Boote, W. D. Batchelor, L. A. Hunt, P. W. Wilkens, U. Singh, A. J. Gijsman, and J. T. Ritchie, 2003: The DSSAT cropping system model. *Europ. J. Agron.*, **18**, 235–265.

Lee, M. H., 2001: Low temperature tolerance in rice: the Korean experience. *ACIAR Proceedings 101; Increased Lowland Rice Production in the Mekong Region*, S. Fukai and J. Basnayake, Eds., Australian Center for International Agricultural Research, GPO Box 1571, Canberra, ACT, 138–146.

Li S. A. 2013: Development of a regional rice model for assessing the impact of climate change on rice in South Korea. APCC Research Report, APEC Climate Centre, Busan, Republic of Korea.

Li, S. A, and A. Tompkins, 2012: The impact of using different temporal and spatial scale average weather data for forecasting of crop, *Climate Res.*, **55**, 65–78.

Li, S. A., T. R. Wheeler, and A. J. Challinor, 2007: Development of a large area wheat crop model for studying climate change impacts in China. *J. Ag. Sci.*, **145**, 47 pp.

Li, S. A., T. R. Wheeler, A. J. Challinor, E. D. Lin, Y. L., and H. Ju, 2010a: Simulating the impacts of global warming on wheat in China using a large area crop model. *Acta. Meteorol Sin*, **24**, 123–135.

Li, S. A., T. R. Wheeler, A. J. Challinor, E. D. Lin, and H. Ju, 2010b: The observed relationship

between crop and climate in China. *Agr Forest Meteorol*, **150**, 1412–1419

Louis, E. A., and E. E. Sunday, 2003: Relationship Between Global Solar Radiation and Sunshine Duration for Onne, Nigeria. *Turk J Phys*, **27**, 161–167.

Matsui, T., and T. Horie, 1992: Effect of elevated CO2 and high temperature on growth and yield of rice. 2. Sensitive period and pollen germination rate in high temperature sterility of rice spikelets at flowering. Jpn. *J. Crop Sci.*, **61**,148–149.

Matsui, T., and T. Horie, 1992: Effect of elevated CO2and high temperature on growth and yield of rice. 2. Sensitive period and pollen germination rate in high temperature sterility of rice spikelets at flowering. Jpn. *J. Crop Sci.*, **61**,148–149.

McCown, R. L., D. M. Freebairn, and C. J. Smith, 2003: An overview of APSIM, a model designed for farming systems simulation. *Eur. J. Agron.*, **18**, 267–288.

Mo, X., S. Liu, Z. Lin, Y. Xu, Y. Xiang, and T. McVicar, 2005: Prediction of crop yield, water consumption and water use efficiency with a SVATcrop growth model using remotely sensed data on the North China Plain. *Ecol Model*, **183**(2–3), 301–322.

Monfreda, C., N. Ramankutty, and J. A. Foley, 2008: Farming the Planet. Part 2: The Geographic Distribution of Crop Areas and Yields in the Year 2000. *Glob. Biogeochem. Cycles*, **22**(1).

Moulin, S., and M. Guerif, 1999: Impacts of model parameter uncertainties on crop reflectance estimates: a regional case study on wheat. *Int J Remote Sens.*, **20** (1), 213–218.

Nichols, N., 1991: Advances in long-term weather forecasting. *Climatic Risk in Crop Production: Models and Management for the Semiarid Tropics and Subtropics*, R.C. Muchow, and J.A. Bellamy, Eds., CAB International, Wallingford, 427–444.

Park, N. S., J. H. Park, and J. Kim, 2012: Development of Korean Paddy Rice Yield Prediction Model (KRPM) using Meteorological Element and MODIS NDVI. *J Korean Soc Agri. Eng.*, **54**, 141–148.

Porter, J. R., and M. A. Semenov, 1999: Climate variability and crop yields in Europe. *Nature*, **400**, 724.

Porter, J. R., and M. A. Semenov, 2005: Crop responses to climatic variability. *Philos Trans R Soc Lond B Biol Sci*. **360**, 2021–2035

Potgieter, A. B., G. L. Hammer, A. Doherty, and P. de Voil, 2005: A simple regional-scale model for forecasting sorghum yield across North-Eastern Australia. *Agric. Forest Meteorol.*, **132**,143–153

Priestly, C. H. B., and R. J. Taylor, 1972: On the assessment of surface heat flux and evaporation using large-scale parameters. *Monthly Weather Rev.*, **100** (2), 81–92.

Ritchie, J. T., 1991: Wheat phasic development. Modelling Plant and Soil Systems, J. Hanks and J. T. Ritchie, Eds., Madison, WI: American Society of Agronomy, 31–54

Rosenthal, W. D., G. L. Hammer, and D. Butler, 1998: Predicting regional grain sorghum production in Australia using spatial modelling. Agric. *Forest Meteorol*. **91**, 263–274.

Rukundo, O., and H. Q. Cao, 2012: Nearest Neighbor Value Interpolation. *Int J Adv Comp Sci Appl*, **3**(4), 1–5

Sacks, W. J., D. Deryng, J. A. Foley, and N. Ramankutty, 2010: Crop planting dates: An analysis of global patterns. *Global Ecol Biogeogr*, **19**, 607–620.

Satake, T, and S. Yoshida, 1978: High temperature-induced sterility in Indica rice at flowering. *Jpn. J. Crop Sci*. **47**, 6–17.

Savada A. M, and Shaw W., 1990: South Korea: *A Country Study*. Washington. GPO for the Library of Congress.

Semenov M. A., and J. R. Porter, 1995: Climatic variability and the modeling of crop yields. *Agric Forest Meteorol*. **73**, 265–283.

Sinclair, T. R., 1998: Limits to crop yield? Plants and population: IS there time? Proceedings of the National Academy of Science Colloquium, Dec, 5–6.

Stöckle, C. O., M. Donatelli, and R. Nelson, 2003: CropSyst a cropping system simulation model. *Europ. J. Agron.*, **18**, 289-307.

Uchijima, T., 1976: Some aspects of relation between low air temperature and sterile spikelets

in rice plants. *J. Agric. Meteorol.*, **31**, 199–202.

Van Ittersum, M.K., P.A. Leffelaar, H. van Keulen, M.J. Kropff, L. Bastiaans, and J. Goudriaan, 2003: On approaches and applications of the Wageningen crop models. *Eur. J. Agron.*, **18**, 201–234.

Wang, X. Y., W. J. Liang, and D. Z. Wen, 2004: Effects of intermittent irrigation on ecological and physiological water requirement of rice in north China. *Chinese J Appl Ecol*, **15**(10), 1911–1915.

Yan, W. K., and D. H. Wallace, 1995: A physiological-genetic model of photoperiod-temperature interactions in photoperiodism, vernalization and male sterility of plants. *Hortic Rev.*, **17**, 73–123.

Yoshida, S., 1975: Factors that limit the growth and yields of upland rice. *Major research in upland rice*, International Rice Research Institute, 46–71.

Yuan, H., Y. Dai, Z. Xiao, D. Ji, and W. Shangguan, 2011: Reprocessing the MODIS Leaf Area Index Products for Land Surface and Climate Modelling. *Remote Sens Environ*, **115**(5), 1171-1187.

Yun J. I. 2003: Predicting regional rice production in South Korea using spatial data and crop-growth modeling. *Agri Syst*, **77**, 23–38.

RESEARCH REPORT 2015-21

Application of the Regional Rice Model GLAM-Rice in the Seasonal Crop Forecasting of South Korea

Sanai Li Climate Change Research Team

APEC Climate Center
12 Centum 7-ro, Haeundae-gu, Busan 612-020, Republic of Korea
Tel: +82-51-745-3900 Fax: +82-51-745-3949

www.apcc21.org

www.facebook.com/apcc21 www.twitter.com/apcc21 www.flickr.com/apcc21
www.youtube.com/APECClimateCenter21 www.plus.google.com/+APECClimateCenter21